UNIVERSIDADE DE LISBOA

Faculdade de Farmácia

Effects on migration of breast cancer cells in 3D models upon MMP inhibition

Susana Duarte Lopes Mascarenhas Proença

Orientadora: Doutora Joana Miranda
Co-orientador: Professor Nuno Oliveira

Dissertação
Mestrado em Ciências Biofarmacêuticas

2016

UNIVERSIDADE DE LISBOA

Faculdade de Farmácia

Effects on migration of breast cancer cells in 3D models upon MMP inhibition

Susana Duarte Lopes Mascarenhas Proença

Orientadora: Doutora Joana Miranda
Co-orientador: Professor Nuno Oliveira

Dissertação

Mestrado em Ciências Biofarmacêuticas

2016

Agradecimentos

Em primeiro lugar quero agradecer aos meus orientadores, Professora Joana Miranda e Professor Nuno Oliveira, por tão bem me integrarem na equipa. Obrigada por me apoiarem, confiarem no meu trabalho e investirem em mim. Ajudaram-me a crescer profissionalmente e pessoalmente.

Quero agradecer também à Madalena Cipriano pelo contínuo apoio e exemplo, essenciais à minha aprendizagem, na implementação de novas técnicas, e pelas discussões científicas. Estou também grata pela tua companhia durante estes longos meses.

Agradeço à Professora Judite Costa por me disponibilizar os compostos [15]pyN_5 [16]pyN_5, essenciais para o trabalho aqui desenvolvido. À Prof. Fátima Cabral pela paciência em ensinar-me a química dos compostos macrocíclicos, pela disponibilidade e pelo sorriso sempre pronto. À Prof. Matilde Castro por no meio de tantas responsabilidades me ter indicado a Professora Joana Miranda e o Professor Nuno Oliveira para orientadores, e pelo interesse que teve neste trabalho.

Aos restantes membros do laboratório, em especial ao Sérgio Camões, Patrícia Guerreiro e Ana Flórido, por terem participado na minha aprendizagem ao longo desta tese e tornarem a estadia no laboratório tão agradável.

Às minhas amigas cá em Portugal e no estrangeiro pela compreensão e encorajamento, e por estarem sempre disponíveis para me animar.

À minha família pelo apoio neste longo ano, por fazerem tudo ao seu alcance para que eu pudesse concretizar os meus objetivos. Em especial à minha mãe pela inspiração, por desde cedo me ter encorajado a lutar pelos meus sonhos, a ter sempre um espírito crítico e me estimular a dar o meu melhor.

Ao Tiago, por sempre acreditares em mim, por tudo o que aprendi contigo e pela tua paciência.

Publications

The studies included in this thesis were presented in the following publications

Abstracts:

Oral Presentation

Proença S, Cipriano M, Cabral MF, Costa J, Fernandes AS, Castro M, Oliveira NG, Miranda J P, *Development of 3D breast cancer models for the evaluation of gelatinase inhibition on cell migration*, XLVI "Sociedade Portuguesa de Farmacologia" Meeting, 2016, Porto, Portugal

Poster Presentation

Proença S, Cipriano M, Castro M, Oliveira NG, Miranda JP*, Development of 3D breast cancer models for the evaluation of gelatinase inhibition on cell migration and invasion*, 7th Post-Graduate iMed.ULisboa Students Meeting, 2015, Lisboa, Portugal

Table of Contents

List of Figures

List of Abbreviations

3D- three-dimensional

[15]pyN_5- *3,6,9,12,18-pentaazabicyclo[12.3.1]octadeca-1(18),14,16-triene*

[16]pyN_5- *3,6,10,13,19-pentaazabicyclo[13.3.1]nonadeca-1(19),15,17-triene*

AKT- protein kinase B

CM2D- Conditioned medium from 2D models

CM3D- Conditioned medium from 3D models

CMT- chemically modified tetracycline (s)

DMEM- Dulbecco modified eagle modified medium

DMSO- dimethyl sulfoxide

EDTA- ethylenediaminetetraacetic acid

ECM- extracellular matrix

EMT- epithelial to mesenchymal transition

FBS- fetal bovine serum

FGF- fibroblast growth factor

LOX- lysyl oxidase

LTBP1- latent TGF-β-binding protein 1

MMPi- MMP inhibitor(s)

MMPs- matrix metalloproteinases

MSS- musculoskeletal syndrome

MTS- tetrazolium salt *3-(4,5-dimethylthiazol-2-yl)-5-(3-carboxymethoxyphenyl)-2-(4-sulfophenyl)-2H-tetrazolium*

PAGE- polyacrylamide gel electrophoresis

PI3K- phosphoinositide 3-kinase

Py-macrocyles - pyridine containing macrocycles

RT- room temperature

SDS- sodium dodecyl sulfate

TIMPs- tissue inhibitors of matrix metalloproteinase

TGF-β- transforming growth factor-β

VEGF- vascular endothelial growth factor

Abstract

Breast Cancer lethality is mostly due to metastization, an event that involves cells migration and invasion, with the latter being dependent of extracellular matrix degradation. Due to metalloproteinases (MMPs) role in migration and invasion and correlation of up-regulation of MMP-2 and 9 (gelatinases) with tumor aggressiveness, these enzymes are considered important druggable targets. 3D models, namely spheroids, have been described as more physiological relevant models. Therefore this work aimed to i) implement breast cancer spheroids model for migration studies; and ii) to evaluate the potential of two pyridine-containing macrocyclic compounds [15]pyN_5 and [16]pyN_5 as MMP inhibitors. The MMP-2 inhibitor ARP-100 was used as control. Spheroids of MDA-MB-231 cells were developed using Matrigel™ in non-adherent culture plates, being monolayer cultures used as controls. During the whole culture time, compact spheroids with diameters of ~200 µm were obtained, containing evenly distributed cells, with different gelatinase secretion when compared to monolayer cultures. The cytotoxicity of the compounds (1-100 µM) was evaluated, through a 24 h tetrazolium-based assay. Cell viability was > 70% for concentrations up to 50 µM of all compounds, in 2D and 3D cultures. The effect of these compounds (1-40 µM) on gelatinases activity was evaluated by a modified zymography technique. For 3D conditioned media both [15]pyN_5 and [16]pyN_5 at 7.5 µM revealed a 100% inhibition of MMP-2/9, while ARP inhibited 52% and 84% of MMP-9 and MMP-2 activity, respectively. Cell migration was analyzed through radial migration and scratch assay for 3D and 2D cultures, respectively. Migration in 2D models was affected ($p<0.05$) by both pyridine-containing macrocycles (5 µM), but not significantly by ARP-100 (up to 40 µM). Radial Migration was less extensively affected, having only significant inhibition for [16]pyN_5 (20 µM) and ARP-100 (40 µM). In the future, invasion assays will be performed to further explore the therapeutic potential of these promising pyridine-containing macrocycles.

Key-Words: 3D models, breast cancer, cell migration, gelatinases, MMPs Inhibitors

Resumo

O cancro de mama foi, em 2012, a 5ª causa de morte por cancro no mundo [1]. A maioria destas mortes deve-se à metastização, facto que se reflete na taxa de sobrevida a 5 anos que em cancros localizados é de 98,6% enquanto em cancro disseminado de mama é de 25,9% [2]. A metastização envolve migração e invasão celular, capacidades que as células tumorais de mama adquirem através da transição epitelial-mesenquimal. Esta transição consiste numa mudança de célula epitelial para uma célula do tipo mesenquimatosa e é caracterizada pela perda dos marcadores epiteliais, nomeadamente proteínas de interação célula-célula, célula-matriz extracelular (ECM), proteínas do citoesqueleto e perda de polarização. Simultaneamente, as células ganham a plasticidade necessária para a migração/invasão [3]. Este processo depende de proteases, entre as quais as metaloproteases de matriz (MMPs), grupo de enzimas dependentes de zinco que clivam elementos da matriz extracelular, entre outras funções [4]. As MMPs, especialmente o grupo das gelatinases (MMP-2 e 9), têm sido bastante associadas a tumores metastáticos e estão correlacionadas com a agressividade de alguns tumores [5]. Dado que as MMPs foram identificadas como possíveis alvos terapêuticos, foram desenvolvidos inibidores destas enzimas. Estes inibidores demonstraram resultados pré-clínicos promissores, mas já em fase clínica mostraram falta de eficácia e efeitos secundários de síndrome musculosquelético. Uma das hipóteses sugerida para este insucesso responsabilizava o grupo quelante de zinco comum a muitos destes inibidores, o ácido hidroxâmico [6]. No nosso laboratório foram sintetizados dois macrociclos do tipo pentaaza contendo um grupo piridina no anel, o [15]pyN_5 e o [16]pyN_5. Estes compostos têm a particularidade de apresentarem constantes de estabilidade elevadas para o catião Zn(II), tendo sido avaliado o seu potencial como inibidores de MMPs e consequentemente da migração celular.

Por outro lado a elevada taxa de insucesso no desenvolvimento de fármacos na área de oncologia, revela a necessidade de ter modelos *in vitro* mais preditivos [7]. Os modelos celulares 3D vêm assim fazer uma ponte entre os modelos animais, mais complexos, e os modelos celulares 2D. Os modelos 3D são fisiologicamente mais relevantes do que os modelos de monocamada por simularem melhor as interações célula-célula, e na presença de ECM, as interações célula-matriz. Estes modelos são especialmente úteis no estudo de cancro dada a importância do microambiente tumoral para a progressão tumoral, incluindo a metastização [8]. Dos vários modelos 3D, os esferoides têm sido dos mais estudados. Estes modelos também são capazes de criar o gradiente de nutrientes e oxigénio que ocorre naturalmente *in vivo*, gradientes importantes para criar uma heterogeneidade de células proliferativas e por vezes até de centros necróticos [9].

Assim sendo, os objetivos deste trabalho foram utilizar a linha celular metastática de adenocarcinoma mamário, MDA-MB-231 para desenvolver modelos 3D. O modelo clássico 2D, foi utilizado como controlo. Nestes modelos testaram-se os compostos [15]pyN_5 e [16]pyN_5 como inibidores das MMPs, especificamente das gelatinases, e estudou-se o seu efeito na migração celular, comparativamente com um inibidor comercial da MMP-2, o ARP-100.

O primeiro passo consistiu em implementar e optimizar os modelos 3D, utilizando placas de baixa aderência para a formação de agregados celulares. Por representar o melhor consenso entre esferoides morfologicamente homogéneos e razão célula/meio que permitisse o condicionamento de meio, escolheu-se um inóculo de 250.000 células/mL, obtendo-se esferoides com uma média de diâmetros de 200 µm. A caracterização de cortes histológicos dos esferoides do dia 4 de cultura, por hematoxilina & eosina, revelaram distribuição homogénea de células, a presença de ECM e ausência de centros necróticos. No entanto, a quantificação de proteína total, o ensaio de viabilidade por MTS e a imunomarcação com Ki-67 revelaram reduzida proliferação. O condicionamento de meio de culturas 2D e de esferóides e subsequente análise dos dois revelaram que os esferóides exibiam maior atividade da MMP-9 do que a MMP-2, contrariamente ao observado nas células em monocamada.

A citotoxicidade dos compostos (1-100 µM) foi avaliada em ensaios de 24 horas com MTS, ensaio baseado na bioredução de um tetrazólio, de forma a selecionar as concentrações a serem usadas nos ensaios seguintes. A viabilidade para ambos os macrociclos contendo piridina revelou-se semelhante nos modelos 3D e nos 2D, não sendo inferior a 70% até 50 µM. Já para o ARP-100, a viabilidade celular no modelo 2D revelou-se mais baixa do que no modelo 3D, com concentrações acima de 50 µM.

Seguidamente, o ensaio de zimografia de gelatina para análise da atividade das gelatinases foi implementado e otimizou-se o condicionamento de meio para a sua análise. A utilização de EDTA confirmou a natureza metalo-proteica das bandas observadas. Havendo a hipótese dos compostos se libertarem das gelatinases durante a eletroforese, fenómeno que ocorre com os inibidores endógenos das MMPs, modificou-se o ensaio de zimografia. A modificação consistiu em colocar os compostos ([15]pyN_5 [16]pyN_5 e ARP-100) em contacto com as gelatinases já após a eletroforese, na fase de degradação gelatinolítica. Desta forma garantiu-se que as diferenças observadas nas bandas resultavam do efeito direto dos compostos.

O teste dos compostos demonstrou que o ARP-100 a 40 µM resultou numa inibição de 100%. No que respeita aos macrociclos, estes não inibiram a actividade gelatinolítica de meio condicionado das culturas 3D a 5 µM, mas atingiram notavelmente, 100% de inibição a

7,5 μM. Esta curva dose-resposta correlaciona com o zinco livre em condições fisiológicas, para ambos os compostos.

O efeito dos compostos na migração celular em 2D foi testado com ensaios de ferida. Este ensaio consiste em fazer um risco numa monocamada confluente e medir a distância entre os extremos da ferida ao tempo 0, e neste caso, às 24 horas, o que indica a migração celular. Para os esferóides, fizeram-se ensaios de migração radial, colocando os esferóides sobre um revestimento de Matrigel™, onde estes aderem. Após 24 horas mediram-se as distâncias entre as células migradas e a superfície dos esferóides. A migração no modelo 2D foi afetada com os compostos macrocíclicos contendo piridina a 5 μM: [16]pyN_5 reduziu 38±2% e [15]pyN_5 reduziu 21±4% da migração. No entanto, o efeito de inibição destes compostos não aumentou com a concentração. O ARP-100 pelo contrário, não demonstrou efeitos significativos de inibição até 40 μM. A migração dos modelos 3D revelou-se assim menos afectada pelos compostos. Os compostos macrocíclicos contendo piridina só demonstraram redução da migração aos 20 e 40 μM, só sendo significativa para o [16]pyN_5 a 20 μM (20±4%). O ARP-100 apenas diminuiu 23±3% da migração celular a 40 μM ($p<0.05$).

Concluindo, os modelos 3D de cancro de mama para o estudo de processos envolvidos na metastização, foram implementados e caracterizados com sucesso. Estes modelos demonstraram diferenças relativamente às células em monocamada. Aqui, reportámos também, que os dois compostos [15]pyN_5 e [16]pyN_5 reduziram a migração em monocamada e, de uma forma mais ligeira, a migração celular nos modelos 3D. Este efeito na migração envolve a inibição da atividade gelatinolítica da MMP-2 e MMP-9, e possivelmente das outras MMPs. Os dois macrociclos contendo piridina aparentaram ser mais potentes nestas funções relativamente ao ARP-100.

Como perspetiva futura, pretende-se testar o [15]pyN_5, o [16]pyN_5 e o ARP-100 na invasão celular, dado o papel das MMPs ser ainda mais relevante neste processo. Também pretendemos investigar o mecanismo de inibição das MMPs com [15]pyN_5 e [16]pyN_5 através de estudos *in silico*.

Palavras-chave: modelos 3D, cancro de mama, migração celular, gelatinases, inibidores de MMPs

1.Introduction

1.1. Breast Cancer

Although much progress has been achieved in breast cancer treatment, efforts applied in cancer research should not diminish. In 2012, breast cancer was the 2nd most diagnosed cancer and the 5th leading cause of dead by cancer worldwide [1], and its incidence is continuously increasing by the dissemination of developed countries risk factors such as aging, overweight, tobacco and alcohol consumption and also hormone treatments and reproductive trends [10]. The improvement made in detection methods allows for earlier diagnosis, preventing tumors progression into more aggressive stages and its metastization, explaining the decrease of breast cancer lethality in developed countries. Adjuvant therapy has also aided in decreasing lethality, but therapies targeting specifically tumor cells migration and invasion steps are still of great demand. In breast cancer, the occurrence of distant metastasis is particularly relevant, as nearly all breast cancer–related deaths are not caused by the primary tumor [10, 11].

1.2. Tumor Cells Migration and Invasiveness and the Role of Tumor Microenvironment

A crucial step for processes such as embryonic morphogenesis and wound healing is the Epithelial to Mesenchymal Transition (EMT), in which cells gain the ability to migrate. It has been found that tumor cells can also advantageously use EMT, allowing them not to be confined to a specific tissue, thus metastasizing to other sites. EMT comprehends the loss of epithelial markers such as tight and adherent junction proteins, e.g. E-cadherin, desmoplakin, occludins and claudins, and intermediate filaments, e.g. cytokeratin-8, 9 and 18, resulting in loss of basal-apical polarity. Alongside, these cells also gain mesenchymal markers N-cadherin, cytokeratin -5 and 14, vimentin, smooth muscle actin and myosin. Some of them are also markers of basal/myoepithelial breast cells. With the acquired plasticity, tumor cells develop protrusions in their leading edge, through actin filaments polymerization, and then form focal contacts by integrin binding extracellular matrix (ECM) proteins. ECM Proteases, such as matrix metalloproteinases (MMPs), are recruited to the leading edge for localized proteolysis of ECM net, clearing away for cell movement which unfolds by myosin-mediated actin filament contraction and simultaneously detachment of the trailing edge by focal contact

disassembly. Cells may migrate individually or collectively, depending on the state of cell-cell adhesions (e.g. cadherins and gap junctions) [reviewed in [3, 12] .

The loss of E-cadherin, which compromises cell-cell-aggregation, is one of the most important events in EMT, such that simply silencing E-cadherin induces this process. Nevertheless, the role of E-cadherin cannot be reduced to a structural function as full EMT was not observed in E-cadherin mutants lacking only its ectodomain [13]. *In vivo,* E-cadherin loss can be due to mutations in its promoter or downregulation by transcriptional factors such as Slug, Twist and Snail [14]. During the E-cadherin depletion, β-catenin, which is sequestered in its cytoplasmic domain, is released. If β-catenin is unphosphorylated, it can activate the expression of EMT-inducing transcriptional factors [13]. GSK3β (Glycogen synthase kinase -3β), the protein responsible for the phosphorylation of β-catenin, has its activity inhibited by hypoxia. In fact, it is long established the importance of hypoxia for tumor progression for its role as an inducer of several EMT-transcriptional factors (e.g. Hypoxia-inducible factor 1-α, Snail and Twist1). Moreover, hypoxia also increases chemotherapeutics resistance [14, 15].

ECM has a major role in mesenchymal migration, not only as a barrier, but also as substrate [3]. Besides its structural function, ECM has been shown to have essential roles in normal and malignant breast tissue development by inducing specific signaling pathways. Indeed, the ECM undergoes structural and composition changes during tumor development, particularly in breast tumor, ECM gains a characteristic stiffness. Levental *et al.* [16] showed that this stiffness can be caused by lysyl oxidase (LOX)-induced collagen crosslinking. This event induces tension-dependent integrin clustering and consequently promotes focal adhesions which increase growth and invasion of premalignant epithelium through Phosphoinositide 3-kinase (PI3K). This increased malignancy was not observed with the inhibition of Lox, PI3K or clusterisation of integrins. Among LOX regulators are transforming growth factor-β (TGF-β) [16] and hypoxia [17].

These examples are just a glimpse of the complex influence that tumor microenvironment has in tumor development. It is also noteworthy that much remains to be clarified about EMT, as there are doubts about its relevance *in vivo*, for not all circulating tumor cells exhibit a mesenchymal phenotype. But again as stated by Li *et al.* [18], EMT “is not a binary process, but instead includes a spectrum of intermediate states that have different degrees of simultaneous expression of epithelial and mesenchymal markers,” and which is probably regulated by redundant pathways. Also, it has been reported a cancer cell line performing “amoeboid” migration, a proteolytic-independent migration, characterized by very few focal contacts cell-matrix [19], which role *in vivo* is still unknown.

1.3. MMPs

As aforementioned, MMPs also have an important role in tumor metastization. In fact, some of these proteinases correlate with increased tumor aggressiveness in primary breast cancer cells and cell lines [5, 20, 21], suggesting a potential role as biomarkers. Furthermore, MMPs have been connected with diseases in the nervous, cardiovascular and respiratory systems, and disorders of the immune system, such as the abnormal tissue proteolysis typical of arthritis [6, 21]. Moreover, MMPs also participate in matrix-cell signal transduction modulation as during ECM degradation, peptides with chemotactic functions are generated, further inducing tumor migration [3, 22]. Also some growth factors, such as fibroblast growth factors (FGF) and vascular endothelial growth factors (VEGF), which are sequestered by the ECM protein, heparin, are released, inducing tumor proliferation, angiogenesis and/or migration [24, 25]. Some of MMPs' roles in regulation of tumor microenvironment, including migration/invasion, are depicted in Fig. 1 [26].

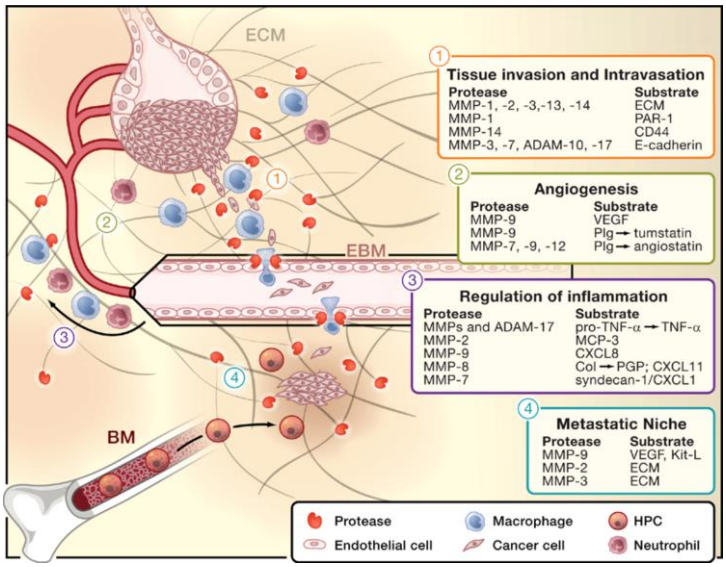

Figure 1. MMPs' regulation of Tumor Microenvironment (EBM-endothelial basement membrane; BM-bone marrow) [26]***.***

MMP constitutes a family of 24 zinc (Zn^{2+}) dependent endopeptidases, which are currently grouped by their ECM substrate and domain organization: collagenases (MMP-1, 8 and 13); gelatinases (MMP-2 and 9); stromelysin (MMP-3, 10 and 11); matrylisins (MMP-7 and 26); membrane type MMPs (MT-MMPs), etc. Despite this nomenclature, it has been shown that MMPs have a substantial substrate overlap and can virtually cleave any ECM

component and in some cases growth factors, cell adhesion molecules and other proteases precursors as well [23, 27].

MMPs catalytic domain is quite conserved, containing a catalytic Zn^{2+} ion (Fig. 2 [22]). They also contain a structural Zn^{2+} ion and one to three Ca^{2+} ions [28]. The catalytic Zn^{2+} ion is coordinated by three histidine residues contained in the conserved motif HExGHxxGxxH and a fixed water molecule, which is simultaneously hydrogen bonded to the protonated carboxyl group of the catalytic glutamic acid residue [29]. The cleavage of the peptide bond, as illustrated in Fig. 2, is mediated by the zinc ion, water molecule and a nearby residue which functions as an hydrogen donor [30]. This catalytic site is flanked by three pockets on the right and left side [31].

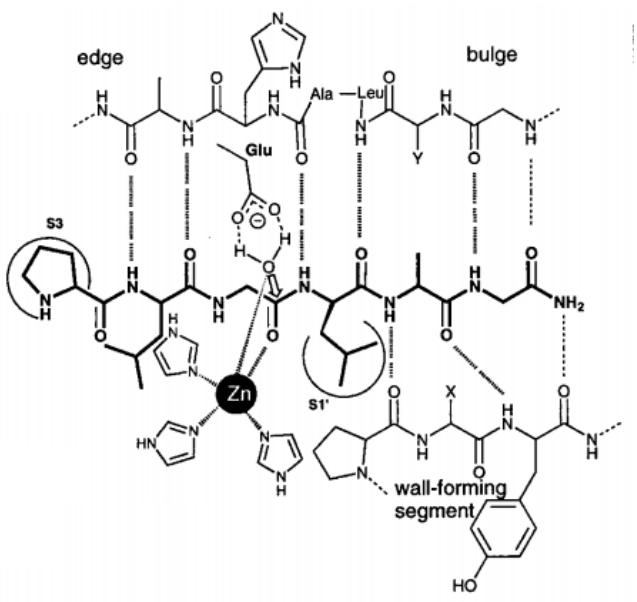

Figure 2. MMP catalytic center with a modeled Pro-Leu-Gly-Leu-Ala-Gly-amide hexapeptide substrate [22]**.**

Another common structure to MMPs is the hemopexin-like C-terminal domain which is essential for non-proteolytic functions of MMPs [26]. Finally, most MMPs also have a highly conserved signal peptide for secretion, and are produced as zymogens, requiring a pro-peptide cleavage for activation, which depending on the MMP can occur intracellularly or extracellularly, and can include different proteins for its activation [20, 23]. This pro-peptide domain contains a conserved “cysteine switch” motif at the N-terminal, in which the sulfhydryl group of the cysteine residue integrates in a tetrahedral coordination sphere with the Zn^{2+} ion, blocking its activity and maintaining enzyme latency [31].

MMP activity is not directly correlated to its expression/secretion as they have endogenous inhibitors, the tissue inhibitors of matrix metalloproteinase (TIMPs). Four TIMPs

have been described in humans with different localization and substrate specificity. Besides this specificity, they still have a considerable substrate overlapping. TIMPS are homologous proteins highly conserved in their immediate N-terminal region through which interacts with the MMPs catalytic domain. A key event in this inhibition is the bidentate coordination of the Zn^{2+} by N-terminal cysteine residue of TIMPs, which displaces the water molecule coordinated by Zn^{2+} from the enzyme [32]. However, because TIMPs can target other proteins than MMPs, their effects are not restricted to the ones directly related to MMP inhibition, having either pro or anti-proliferative, and even anti-apoptotic effects which makes their role in cancer ambiguous. In fact, TIMP-1 correlates with lung metastasis and breast cancer stage [21, 33]. As neither the expression of TIMPs can be completely correlated to MMP activity, nor their effects are solely anti-tumorigenic, they are not greatly considered as a possible therapy target.

Similarly, although initially was thought all MMPs had a detrimental effect on cancer, the opposite was shown, with some MMPs presenting beneficial roles in cancer [6]. Hence, targeting MMPs' for therapy should be carefully addressed as further studies on their functions should be made.

Gelatinases (MMP-2 and 9)

MMP-2 and MMP-9, gelatinases A and B, respectively, are some of MMPs that have a higher correlation with metastatic cancer and are indicative of worse prognosis [34, 35]. MMP-9 correlation with the stage of cancer is particularly strong, being shown in one epidemiological study that the concentration of this protein decreased after surgical removal of the tumor. This concentration remained low increasing again only 1 to 8 months before diagnosis of recurrence for 20% of patients. It even correlated to the cases in which there was a lack of response to therapy [36]. However, in tumor microenvironment, not just tumor cells are responsible for MMP-2/9 production. Breast cancer cells MDA-MB-231 were able to release MMP-2 bound to non-malignant fibroblasts membrane [37] and it was shown that neutrophils synthesis and secretion of MMP-9, has an important role in tumor progression [38].

Although MMPs are highly homologous proteins, gelatinases have a unique domain, the fibronectin type II repeats (Fig. 3 [23]), which aids in the binding to fibronectin, gelatin or collagen for their cleavage. Selectivity has been a major focus in terms of MMP inhibitors design. In this sense, a big emphasis to the S1' pocket was given as it was the one differing the most among MMPs. This pocket is hydrophobic, more in MMP-2 than 9, and is open with no significant interactions. The major difference between MMP-9 and 2 is a loop present in the former and not in the last [29].

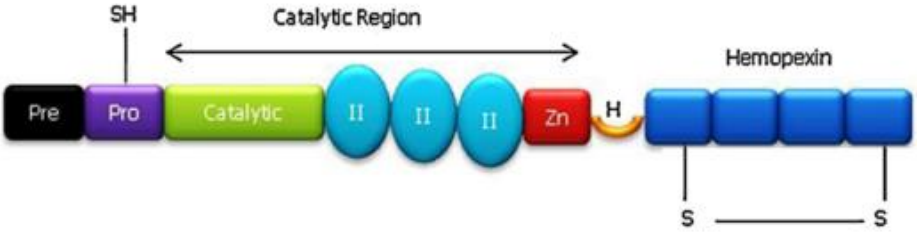

Figure 3. Gelatinases basic domain structure [23]*. Common to MMPs: Pre-peptide signal, Pro-propetide domain; Zn- highly conserved zinc-binding site; H- Hinge region linking the Hemopexin-like domain to the catalytic domain (not existing in MMP-2); Specific for gelatinases: II-fibronectin type II repeats.*

MMP-2 pro-form of 72 kDa can be proteolytically activated to a 66 kDa form, by MMP-1, 7, thrombin and TIMP-2. TIMP-2 interacts through its C-terminal with MMP-2 hemopexin domain and through its N-terminal with MT-MMP1 (MMP-14). The MMP-2 pro-domain is then cleaved when a second MT-MMP-1 joins the complex and interacts with the first MT-MMP1 hemopexin domain. Although TIMP-3 and TIMP-4 can also form these complexes, by not allowing cleavage of pro-MMP-2, they act as inhibitors of the complex. The activated MMP-2 in its turn can activate other MMPs such as MMP-9, MMP-1 and MMP-13 [27, 39, 40]. Moreover, the 92 kDa pro-MMP-9 can be activated to a 83 kDa form by plasmin, trypsin 2, MMP-3 and MMP-13 [23, 40].

The MMP-9 is also the only MMP known to form homodimers, by their hemopexin domains binding. These homodimers have been associated to CD44 complex, which is thought to protect MMP-9 from inhibition by TIMP-1 and to have a role in migration/invasion perhaps more relevant than MMP-9 monomers [41].

Despite their name, gelatinases also cleave other ECM proteins, such as collagen type IV, V, VII, IX and X [23]. The gelatinase substrates also include molecules with signaling functions. For example, gelatinases were shown to activate TGF-β by proteolytic activation of pro-TGF-β, and also by releasing it from latent TGF-β-binding protein 1 (LTBP1), an ECM protein [42][43]. Although TGF-β has dual roles in cancer, some cancer cells gain mutations that turn them insensitive to TGF-β tumor suppressive arm, but keep TGF-β pro-tumor functions involved in EMT, tumor growth, etc. [44]. In a similar manner, TIMP-free MMP- 9 releases VEGF and FGF-2 bound to the ECM [38, 45] promoting angiogenesis. MMP-2 induces VEGF expression, by interacting with integrin αVβ3 that activates PI3K/Protein Kinase B (AKT) pathway and transcription factors downstream, such as HIF-1α. VEGF in turn, further induces MMP synthesis [46]. Indeed, Nakamura *et al.* [47] showed that administration of a MMP-9 and 2 inhibitor MMPi270, decreased lymph node metastasis and *in vitro* presented inhibition of lymphangiogenesis properties such as invasion and tube formation. For migration/invasion specific pathways it was reported that MMP-9 induced expression by

Epithelial Growth Factor Receptor (EGFR) caused the loss of E-cadherin [48] which, as herein earlier described, is a fundamental step in EMT. Also, during ECM proteolysis, MMP-9 and MMP-2 produce peptides with chemotactic effects, such as the N-terminal ectodomain of Ninjurin1 [49] and Laminin 5γ2 fragment [50], respectively. However, it is noteworthy the ambiguous role that gelatinases, as other MMPs and TIMPs have. Potent suppressors of angiogenesis, angiostatin and a monomeric NC1 domain, result from the degradation of plasminogen and collagen IVα3, respectively, by MMP-9 [51, 52]. Tumors with sizes over 500 mm^3, in MMP-9-deficient mice had accelerated growth relative to control, correlating to low tumstatin [52]. Moreover, MMP-9 promoted an anti-tumor immune response, including massive neutrophils infiltration and significantly induced tumor regression in mice models [53].

1.4. Exogenous MMP Inhibitors (MMPi)

The role of MMPs in tumor development lead to the creation of several MMP inhibitors. The first class of inhibitors consisted of peptidomimetics, compounds which contained pseudopeptides that mimic peptidic bonds, inhibiting MMP action by reversible competitive inhibition, occupying the substrate site and chelating zinc. Due to the MMP promiscuity, by mimicking the collagen MMP's cleavage site, these compounds have a relatively broad action [23, 54].

Many zinc-binding groups such as aminocarboxylates, sulfhydryls and derivates of phosphoric acid have been tested for MMP inhibition [54]. However, by having a stronger binding with MMPs, creating hydrogen bonds with residues of Glu and Ala, conserved aminoacids of MMPs catalytic site, the hydroxamates derivates were the ones receiving more focus with more of these compounds entering clinical trials [55]. Batimastat was the first MMPi entering clinical trials but had limitations in its administration route due to solubility issues [56]. The next generation of these compounds, such as marimastat, in Fig. 4, were soluble enough to allow oral administration [57, 58]. Despite showing very promising pre-clinical data, when used in clinical trials marimastat failed to increase overall survival and induced musculoskeletal syndrome (MSS) side effect that also characterized treatments based on other MMPi [59]. Although specific inhibition of some MMPs such as MMP-1 was indicated as a possible cause for MSS, it was latter disproven [60, 61]. The next generation of inhibitors was developed taken into account these proteins whose structures were then resolved by crystallographic methods. The aim was to develop more specific compounds that could surpass the first generation problems, regarding lack of efficiency and harmful side effects [6, 31]. Being chelating agents, MMPi may off-target non-MMP metal-dependent proteinases [61], hampering a full understand of their effects. Besides, as within MMPs, gelatinases have been indicated as especially important for metastization, molecules more specific for MMP-2 and 9, were

developed. CGS27023A (Novartis) was designed containing an arylsulfonyl group adjacent to hydroxamate, which increased the affinity for gelatinases S1 pocket, and thus, its specificity. Prinomastat (Pfizer) (Fig. 4) was developed following CGS27023A rational, with increased specificity as it contained a diphenylether more suitable for “deep pocket” MMPs [62]. Yet, both compounds still maintain some of the first generation MMPi MSS side effects and therefore, a translation of the pre-clinical success to clinical trials was not observed.

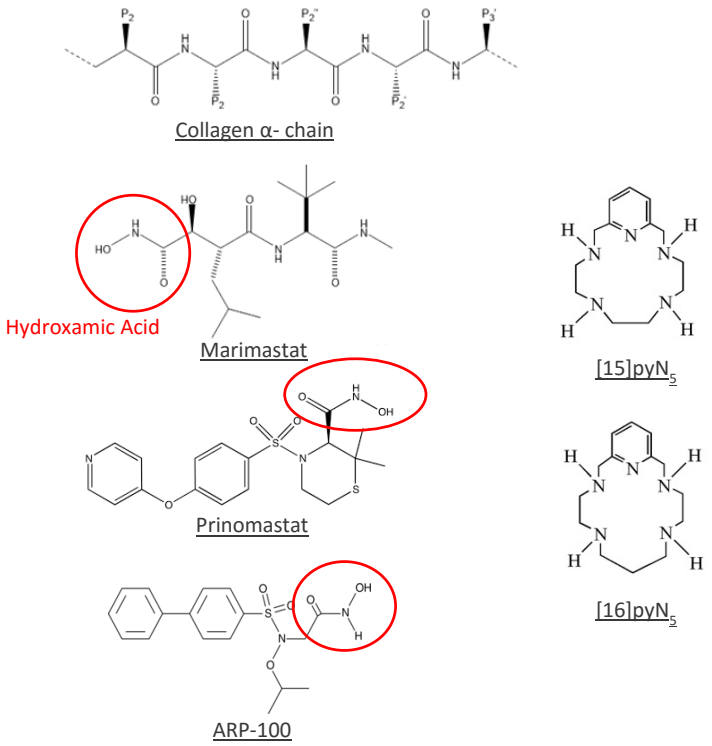

Figure 4. Chemical structure of some hydroxamic acid MMP inhibitors (Marimastat, Prinomastat and ARP-100) and of the macrocyclic compounds containing pyridine ([15]pyN$_5$ and [16]pyN$_5$).

Brown *et al* [63] developed a mechanism-based inhibitor, SB-3CT, with increased specificity for gelatinases. Its specificity for MMP-2 may be due to the induction of pro-MMP-2 like conformation by directly coordinating the catalytic zinc ion to the sulfur atom of the bound inhibitor, forming a tetrahedral coordination at the zinc ion [64]. This mechanism-based inhibitor was shown to successfully inhibit ethanol induced *in vitro* invasion of breast cancer cell lines [65], liver metastasis and to increase survival in an aggressive mouse model of T-cell lymphoma [66].

Using as structural model the arylsulfonamide group contained in prinomastat, CGS-27023A and retrohydroxymate-based ABT-518, Rosselo *et al.* [67, 68] developed a set of new molecules screened for MMPs inhibitory activity. ARP-100 (compound then denominated 10a), which is illustrated in Fig. 4, showed to be the most promising considering both its

potency for MMP-2 inhibition but also selectivity for this MMP over MMP-1, 3 and 7. This selectivity was obtained by adding an alkyl substituent at the carbon atom adjacent to the hydroxamic acid, which added lipophilic interactions to the S1 region of the active site. Consequently, ARP-100 was tested in HT1080 (fibrosarcoma cell line), inhibiting in ~60% of invasive cells (observed by formation of protrusions) in Matrigel™ layered plates (50 nM) [67]. ARP-100 was also tested as a gelatinase inhibitor in A549 lung cancer cells (50 and 100 μM) as a pharmacological control of MMP-2 siRNA [46], and in a co-culture of SKOV3 cell line with primary non-tumor fibroblasts (20-100 nM), where it inhibited adhesion and invasion [69].

Besides these specifically designed compounds, some other old drugs, such as biphosphonates [4, 70] and disulfiram [71] revealed MMPi activity. For disulfiram, mechanisms such as decreasing the DNA binding activity of AP-1 and NF-κB, that diminish tumor invasiveness, have been shown [72].

Amongst natural compounds, curcumin has shown anti-carcinogenic properties. Such properties have been attributed to the inhibition of MMP-2 and 9 in MDA-MB-231 cells through TIMP-1 and 4 up-regulation, and by inducting apoptosis and p21 expression's regulation, through a p53-dependent pathway [73]. Also neovastat (AE-941), a water soluble extract from shark cartilage, was shown to inhibit tumor growth and progression *in vivo* through several mechanisms including MMP-2, 9 and 12 inhibition and VEGF receptor competitive binding. Although in some clinical trials neovastat has improved survival (16.3 versus 7.1 months) in refractory renal cancer cell patients [74], no difference was observed between neovastat and a placebo in incurable breast or colorectal carcinoma [75].

Moreover, after being discovered that tetracyclines and their semisynthetic analogues could inhibit collagenases [76], derivates of these molecules were produced for just this effect. Their antimicrobial activity was chemically removed and these chemically modified tetracyclines (CMT) [77] were evaluated for tumor therapy, with CMT-3 (COL-3 or metastat) having the highest anti-tumorigenic potential. Besides gelatinases' activity and expression inhibition [78], CMT-3 can induce apoptosis in tumor cells from 2 to 8-fold more cytotoxic than doxycycline, both in a caspase dependent and independent pathway and arrest cells at G0/G1 phase [79, 80]. After showing promising pre-clinical results, by decreased the number of metastasis [79] and delaying tumor growth in rat models [81], CMT-3 entered clinical trials. Currently, it is in phase III for Kaposi's sarcoma and in phase I for advanced cancer. No musculoskeletal side effects have been reported yet [21] .

Finally, one of the long lasting problems that has cursed MMPi clinical trials is the design of the clinical trials itself [82]. As aforementioned, MMPs influence in increasing malignancy is a quite early event in tumor development and thus pre-clinical data in early-stage tumors was overall successful. As an example, treatment with batimastat in rats, starting 2 days prior to tumor surgery until 70th day, resulted in 100% survival after the death of all rats

in control group [83]; contrasting with the clinical trials which are based on treatment of patients with advance staged tumors.

Macrocycles as MMP inhibitors

Macrocycles have been potentially described as more specific than open chain chelators, for its ring rigidity which constrains the type of metal it can coordinate [84]. The macrocycle [12]aneN_4 (cyclen) has such a specificity for zinc, that coupled to a fluorophore it works as zinc sensor to detect apoptosis [85]. Therefore, in order to develop new compounds with MMP inhibitory activity, nitrogen-based zinc binding groups, such as macrocycles, have been described. Jacobsen *et al.* [86] showed that relatively to one of the most common zinc binding groups, acetohydroxamic acid (AHA), macrocycles [9]aneN_3, [12]aneN_4 and [14]aneN_4 have improved MMP-3 inhibition potency by 185, 139 and 19-fold (IC50), respectively. Besides, macrocycles were also much more selective than AHA, as they did not inhibit the non-heme iron enzyme soybean lipoxygenase. In contrast, coupling macrocycle compound cyclam to marimastat showed no advantages [87].

In our laboratory, (Chemical Biology and Toxicology, Faculty of Pharmacy, Universidade de Lisboa) [88], two pentaaza-macrocycles containing pyridine in their backbone, [15]pyN_5 and [16]pyN_5 (Fig. 4), were synthesized and have shown high stability constants for Zn^{2+}. Moreover, [15]pyN_5 complexed with Cu^{2+}, has been studied as a superoxide mimetic modulating ROS. This activity was shown to be very promising for cancer treatment as it protected MCF-10A (non-malignant cell line) from oxiplatin treatment in detriment of further inducing death in cancer cell line MCF-7 [89], and to inhibit cell migration and invasion when co-administered with doxorubicin [90].

1.5. Three dimensional models in tumor migration/ invasion assays

With oncology being one of the areas with higher attritions in drug development, one should take a critical look on the models mostly used in pre-clinical phases as they may not be translating the *in vivo* situation [7, 91].

It has been broadly described microenvironment factors (e.g. ECM, stromal cells and gradients of nutrients/ gases) playing crucial roles in tumor development. Therefore, it is reasonable that the development of models, which better represent the interaction of these elements, are essential to obtain more accurate predictions of *in vivo* cells behavior. Although animal models partly represent this complexity, they are also expensive, time consuming, raise ethical issues and do not represent human systems idiosyncrasies. Besides, specifically for tumor context, animal models do not contain the natural tumor cells heterogeneity, and the

animals are frequently immunodeficient. As for *in vitro* models, the current gold standard are cell culture monolayers, in which cells adhere to plastic surfaces, have no gradients of nutrients and oxygen, and have minimal cell-cell interactions. In this context, three dimensional (3D) models of tumor cells emerged as a better alternative by making a bridge between *in vivo* and *in vitro* monolayers models [8, 92]. The most widely studied and characterized 3D model are spheroids which consist in compact cell aggregates that recapitulate *in vivo* cell-adhesion profile inducing reduced proliferative rates relative to monolayers [92]. Besides the three-dimensionality of cell-cell adhesion, spheroids frequently contain ECM elements either by tumor cells intrinsic production or by addition reconstituted extracellular matrix such as hydrogels derived from natural sources [92]. Among these, cell adhesion molecules β-integrins and E-cadherin have critical roles in resistance to chemotherapeutics [93, 94] and overall, in malignancy. Weaver *et al.* [95] has shown that a tumor cell line overexpressing β1-integrin, had its phenotype reversed to a less-malignant one both in 3D and *in vivo* models, by treatment with anti-β1 integrin antibody.

Moreover, spheroids mimic the gradient of nutrients and oxygen that occurs in avascular tumor nodules. By being able to develop an hypoxic region and even necrotic cores, spheroids can give rise to distinct cell populations: proliferating, quiescent and necrotic [96]. Heterogeneity is of extremely importance for chemotherapeutics screenings as the quiescent population often is the cause of chemoresistance. It has been shown by *Mellor et al.* [97] that tumor spheroids of quiescent cells exhibited more resistance to common chemotherapeutics cisplatin, doxorrubicin, 5-fluorouracil and vinblastine than tumor spheroids composed of proliferating cells.

All together these microenvironment factors differentiate cells in spheroids from cells in monolayers. Spheroids of human and mouse tumor cell lines demonstrated transcriptomic differences in two enzymes involved in mitochondrial metabolism and redox reactions enzymes and downregulation of a DNA mismatch repair enzyme (PMS2 gene), enzymes associated with acquired resistance to alkylating agents [98]. Transmembrane proteins also suffer changes, as spheroids of MDA-MB-231 cells show β1-integrins [99] and CD44 [100] upregulated. Moreover breast cancer spheroid models have shown higher expression of ALDH1, MMP1 [100] and urokinase (Upa) [94]. For presenting more stemness-related traits and proteins associated to metastization, spheroids respond differently than monolayers to compounds targeting EMT [101]. Spheroids of non-malignant breast cancer cells which develop an acinar morphology also showed MMP-9 important role in the epithelial polarization disruption [102], possibly by interfering with laminin 111, a molecule previously shown to be essential for normal acinar morphogenesis [103]. This MMP-9 activity was translated to *in vivo* as its silencing in malignant cells T4-2, hampered their tumorigenic ability in mice [102].

Therefore, spheroids are considered very suitable models also for migration/invasion studies [94, 104, 105].

Although 3D models offer more technical difficulties than 2D, they have in fact been fulfilling their potential. Bissel *et al.* [106, 107] have shown the importance of microenvironment factors on normal and malignant breast tissue development, a groundbreaking work that could hardly be done without 3D models. Moreover, in spite of their complexity, they are still *in vitro* models and so high-throughput platforms of 3D models have been developed for chemotherapeutic compounds screenings [101, 104, 108].

2. Aims and experimental models

The global aim of this work was to develop more physiologically relevant 3D model of metastatic breast cancer, to evaluate the effect of potential MMP inhibitors (MMPi) on cell migration.

MDA-MB-231, a triple negative cell line, obtained from a pleural effusion of an breast adenocarcinoma was herein used. MDA-MB-231 cells are metastatic, having both migration and invasion potential, and detectable MMP-2 and MMP-9 secretion [5]. Although there are a variety of methods to create spheroids, herein non-adhesive plates seemed the most suitable. In parallel, monolayers were used as controls.

Following the hypothesis that the MSS side effects and lack of efficiency from the earlier MMPi were due to the zinc-binding group, hydroxamic acid, testing alternative zinc-binding compound was the next step. Therefore, in this work two pyridine-containing macrocyclic compounds, [15]pyN_5 and [16]pyN_5, were suggested as MMP inhibitors. The inhibitory activity of these compounds was evaluated by applying a zymography gel technique with gelatin substrate. These compounds were compared with the commercially available MMP-2 pharmacological inhibitor, ARP-100, which contains the classical zinc-binding group. Moreover, [15]pyN_5, [16]pyN_5 and ARP-100 effect on cell migration was evaluated through a radial and scratch migration, for 3D and 2D cultures, respectively.

3. Methods

3.1. Chemicals

A 40 mM stock solution of ARP-100 (Santa Cruz Biotechnology) was prepared in DMSO (Sigma-Aldrich®). Working solutions were performed so that in each final solution, the DMSO concentration was kept at 0.25% (v/v). Macrocyclic compounds [15]pyN_5 and [16]pyN_5 were dissolved in water at a concentration of 2 mM.

3.2. Maintenance of MDA-MB-231 cells in monolayer cultures

MDA-MB-231 cells, a human breast carcinoma cell line (ATCC), were inoculated at cell densities ranging from 30,000-150,000 cells/ml and cultured in Dulbecco's modified Eagle's medium (DMEM) (Sigma-Aldrich®) supplemented with 10% fetal bovine serum (FBS) (Gibco®, ThermoFisher Scientific). Cultures were kept at 37 °C, under a humidified atmosphere at 37 °C, 5% CO_2-in air.

3.3. Multicellular Spheroids Formation and Maintenance

For spheroid generation, 6-well, 24-wells and 96-wells ULA flat-bottomed plates (Corning® Costar®) were inoculated with 1500 µL/well, 300 µL/well and 50 µL/well, respectively, of cell suspension at the optimized density of 250,000 cells/mL Spheroids culture medium consisted in DMEM supplemented with 10% FBS and 2% Growth Factor Reduced Matrigel™ (Corning®). Twenty-four hours for 6 and 24-wells plates and 2 h for 96-wells plates after inoculation, the volume of culture medium was doubled. Spheroids were incubated for up to 6 days with medium replacement every 3 days, in a humidified chamber at 37°C, 5% CO_2. A scheme of spheroids formation is depicted in Fig. 5.

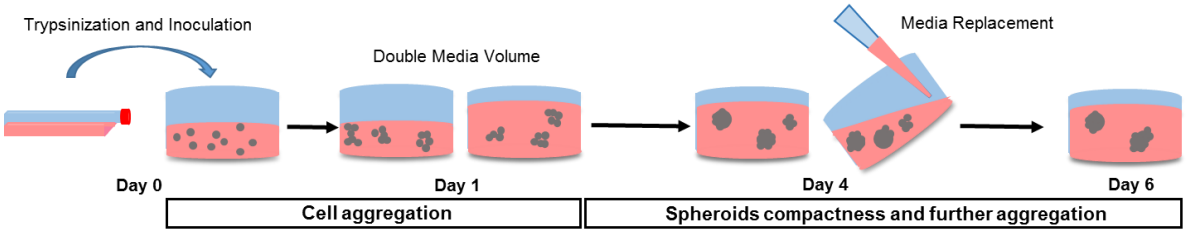

Figure 5. Schematic representation of spheroids culture procedure.

3.4. Histology

3.4.1. H&E

Day-4 spheroids were resuspended in Tissue Tek® O.C.T.™ (Sakura®) for preparing cryosections of 5-7 µm. Slides were first stained with Harris's haematoxylin (Sigma-Aldrich®) for 20 min, followed by Eosin Y (Sigma-Aldrich®) staining for 2 min. Slides were then submitted to increasing concentrations of Ethanol and finally incubated in xylene (EMD Chemicals). Samples were mounted with Entellan® (Merck). Images were acquired on an Olympus CK30 inverted microscope using Motic Images Version 2.0 software.

3.4.2. Ki67

Spheroid cryosections were fixed with pre-cooled acetone for 30 min at -20 °C, left drying and then, permeabilized with 0.08% Tween 20® for 2 min at room temperature (RT) and blocked for 30 min with 2% bovine serum albumin (BSA) in PBS. Incubation with primary antibody was performed overnight (ON) in a humidified chamber at 4°C. The primary antibody used was: Ki67 (Rabbit IgG, AB16667, Abcam®) diluted 1:100 In 1% BSA in PBS. The incubation with the secondary antibody goat anti-rabbit 594 (1:500) (Invitrogen™) was carried out for 1h at RT. Sections were mounted using ProLong gold antifade with DAPI (4',6-diamidino-2-phenylindole, Invitrogen™) and observed on an inverted fluorescence microscope (Axiovert 200M, Carl Zeiss) coupled with a monochrome camera (AxioCam MNC, Carl Zeiss). Sample fluorescence was examined at excitation/emission wavelengths of 590/617 nm (Alexa Fluor 594) and 358/461 (DAPI). Images were collected using AxioVision Rel. 4.7 software.

3.5. MMPi Viability Assays

The cytotoxicity of ARP-100, [15]pyN_5 and [16]pyN_5 was evaluated in MDA-MB-231 cells in 2D and 3D culture conditions using CellTiter 96® AQueous One Solution Cell Proliferation Assay (Promega). In 2D cultures, $8x10^3$ cells were seeded in 96-well plates and maintained for 24 h in DMEM supplemented with 10%FBS. Thereafter, cells were exposed to 100 µL of ARP-100, [15]pyN_5 and [16]pyN_5 in final concentrations 100, 75, 50, 25, 10, 5, and 1 µM, in serum free DMEM. After 24 h incubation, 20 µL MTS was added to the wells and left incubating for 1 h. The absorbance was recorded by spectrophotometry at 490 nm and 690 nm (SPECTROstar Omega, BMG LABTECH).

For 3D culture conditions, spheroids cultured in 96-welll ULA plates were used. Four-day spheroids' culture medium was replaced by 100 µL of DMEM with 1,25% FBS, 2% Matrigel™ and ARP-100, [15]pyN_5 and [16]pyN_5 (100, 75, 40, 10 and 1 µM). After 24 h,

spheroids were incubated 1 h with MTS. Spheroids were pelleted and the supernatant read by spectrophotometry at 490 nm and 690 nm.

The number of surviving cells was assessed by the determination of the difference of absorbance, $A_{490\ nm} - A_{690\ nm}$ and cell viability was expressed as percentage to control. Experiments were performed in triplicates.

3.6. Media Conditioning

For medium conditioning under 2D conditions (CM2D), 1,500,000 cells were seeded in 75 cm^2 T-flask for 24h reaching a 50% confluency. After washing twice with PBS, 15 mL serum-free DMEM was added to the cells. 3D medium conditioning (CM3D) was performed at day 4 of culture, in 6-well ULA plates. Spheroids were washed twice with serum-free DMEM, and medium substituted by 2 mL serum free DMEM supplemented with 2% Matrigel™. For both culture conditions, medium was conditioned for 24 h after which, it was harvested and concentrated about 100X in 10 kDa centrifugal concentrators (Millipore). Total protein was quantified by spectrophotometry (SPECTROstar Omega, BMG LABTECH) in a low volume microplate (Lvis plate, BMG LABTECH). Total protein concentration was determined through Lambert-Beer equation, with absorbance 280-340 nm and extinction coefficient of bovine serum albumin.

3.7. Modified zymography assay

To screen MMP-2 and 9 total gelatinase activity, a sodium dodecyl sulfate Polyacrylamide gel electrophoresis (SDS-PAGE), with the gel containing gelatin as substrate, was performed using the methodology described in [109] with modifications (Fig. 10). CM concentrated samples were resolved by electrophoresis under non-reducing conditions, in a 10% Polyacrylamide containing 0.1% SDS and 0.1% (w/v) Gelatin. After electrophoresis, lanes were individualized and washed with 2.5% Triton X-100 in 3 steps of 20 min, to remove SDS. Lane gels were incubated for 24 h at 37 °C in, the Developing Buffer (50 mM Tris Base, 200 mM NaCl, 5 µM $ZnCl_2$, 5 mM $CaCl_2.2H_2O$ and 0.02% NaN_3) which restores the MMPs protease activity. ARP-100, [15]PyN_5 and [16]pyN_5 were tested by dissolving them in the Developing Buffer. Gels were revealed in 0,1% Coomassie Blue R-250 (National Diagnostics). MMP activity was detected as a clear band in the background of uniform staining. Band quantification was performed using ImageJ software (National Institutes of Health, USA).

3.8. Migration Assays

3.8.1. Scratch Assay

In vitro scratch assays were performed according to Liang *et al.* [110]. Briefly, 200,000 MDA-MB-231 cells were seeded in 24-well plates. After 24 h incubation, medium was removed and a scratch performed with a 200-µL pipette tip, leaving a gap of approximately 0.7 mm in width. Cells were then rinsed twice with PBS and kept in serum-free medium containing 5-40 µM of ARP-100, [15]pyN_5 and [16]pyN_5. The scratch was evaluated microscopically (Motic AE 2000 inverted microscope), and four images of each scratch were recorded using Moticam 2500 at defined time-points: 0, 5, and 10 and 24 h. Non-invaded distance was measured using Motic Images PLUS v2.0 software. Experiments were performed in triplicates.

3.8.2. Radial Migration

This assay was performed according to Vinci *et al* [104]. Flat-bottomed, 24-well plates (Sarstedt) were coated with 0.01 mg/mL with Poly-D-Lysine (Sigma-Aldrich®) in sterile water for 2 h at RT, followed by 1:30 diluted Matrigel™ coating for 30 min. Four-day spheroids were transferred to pre-coated plates and maintained in 500 µL of medium containing 10% FBS and 2% Matrigel™ and the compounds, ARP-100, [15]pyN_5 and [16]pyN_5 in concentrations ranging from 5-40 µM. Images were captured at 5, 10 and 24 h Motic AE 2000 inverted microscope. Effects of compounds were analyzed by measuring the distance between cells in the migration front and the perimeter of the spheroid. More than 10 spheroids per condition were analyzed, with 3 measures per spheroid.

3.9. Statistical analysis

Statistical analyses were carried by GraphPad Prism v6.0 software, (La Jolla, CA, USA). ANOVA with Tukey's multiple comparison post-test was performed for 3 or 4 independent assays. Anova repeated measures tool was used when there were values matching. Results are presented as means ±standard error of the mean (SEM), except where indicated. Statistical significance was represented as probability (p) value *<0.05, **<0.01 and ***<0.001.

4. Results and Discussion

4.1 Development of 3D Models of MDA-MB-231

A suspension culture system using Ultra-Low Attachment (ULA) plates was developed and optimized in order to obtain MDA-MB-231 3D spheroids. ULA plates consist of plates coated with a hydrophilic and neutrally charged hydrogel that prevents cell adherence to the wells surface, therefore promoting cell aggregation. For this purpose, different culture parameters such as inoculum concentration, FBS concentration and ECM supplementation were evaluated. MDA-MB-231 cells were cultured in 24-well plates for 6 days in a batch mode consisting of culture medium replacement every 3 days (Fig. 5).

Medium supplementation with both 10% and 20% FBS, did allow formation of cell aggregates. However, these aggregates were easily disrupted and were heterogeneous in size and morphology (Fig. 6 A). To obtain more compact spheroids of MDA-MB-231 cell line, previous reports [111] recommend the addition of a reconstituted basement membrane. Matrigel™ [112], which is a commercially available basement membrane preparation extracted from the Engelbreth-Holm-Swarm (EHS) mouse sarcoma, rich in ECM proteins (e.g. laminin, collagen IV and heparin sulfate proteoglycans), was therefore added to the 10% FBS cultures at the inoculation step. Indeed, as shown in Fig. 6 B, 2% Matrigel™ allowed the formation of more compact and homogenous spheroids. Consequently, the 10% FBS condition with 2% Matrigel™ was further adopted.

According to previous reports [96, 111] cell densities ranging from 125,000 to 315,000 cell/mL were initially tested (Fig. 6 B). Twenty-four hours were given for cells aggregation, after which media volume was doubled. Measurements of spheroids were based on phase-contrast images up to day 6 of culture, yielding a size-distribution plot (Fig. 6 C).

With the higher inoculums (315,000 cells/mL), larger but more heterogeneous spheroids were obtained. As for the inoculum concentrations of 125,000 and 250,000 cells/mL, homogeneous spheroids were observed from day 4 onwards. However, in order to obtain a conditioning medium volume per cell in 3D cultures as in the two-dimensional system (further explored in Chapter 4.3.1.), the inoculum of 125,000 cells/mL was considered inadequate as it would require a very low cell confluence for medium conditioning in the 2D model. Therefore, for MDA-MB-231 spheroids development, the condition with cell density of 250,000 cells/mL in media supplemented with 10% FBS and 2% Matrigel™ was adopted and further characterized up to day 4.

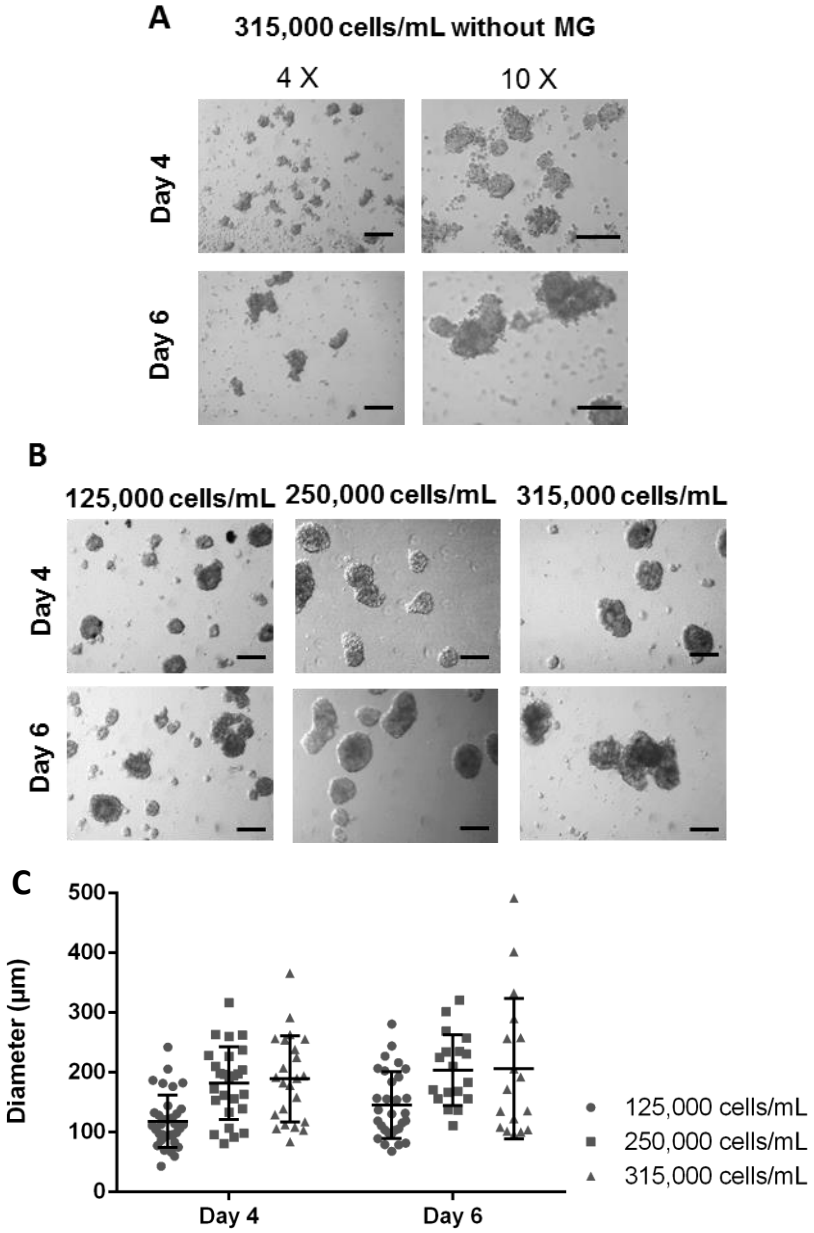

Figure 6. Optimization of MDA-MB-231 spheroids development conditions. *A) Contrast phase pictures of aggregates formed without Matrigel™ (MG), from inoculum 315,000 cells/mL, at day 4 and 6 of culture (magnification 4X, scale bars=200 µm; magnification 10X, scale bar=100 µm). B) Contrast phase pictures of spheroids with 2% Matrigel™ from inoculums 125,000; 250,000 and 315,000 cells/mL at day 4 and 6 of culture (magnification 4X, scale bars=200 µm) Pictures taken with inverted microscope. C) Distribution plot for spheroids diameters (µm) at day 4 and 6 of culture of cells inoculated at 125,000; 250,000 and 315,000 cells/mL.*

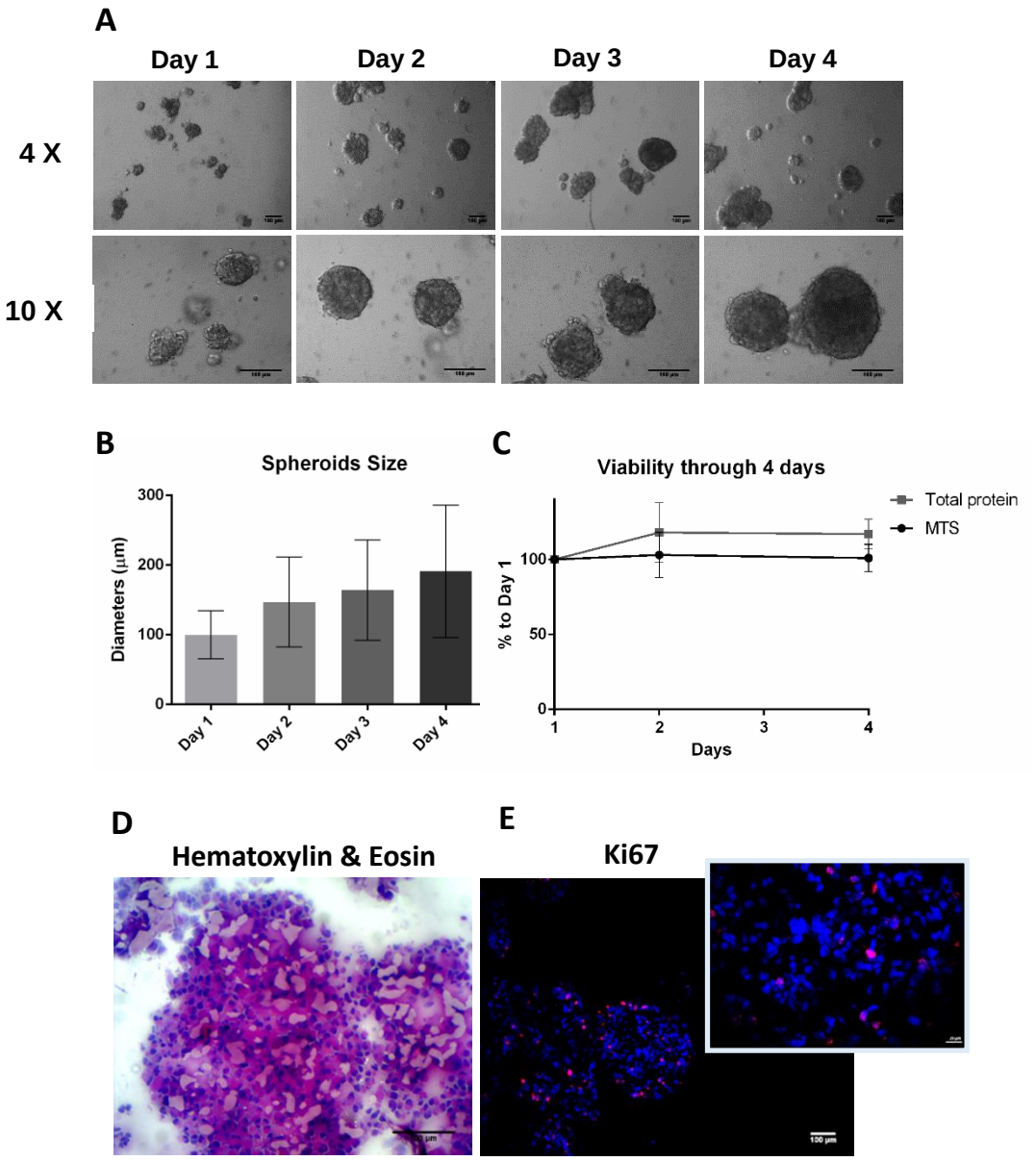

Figure 7. Characterization of MDA-MB-231 spheroids (inoculum 250,000 cell/mL in 10% FBS and 2% Matrigel™ supplemented media). *A) Representative phase contrast images of the spheroids from day 1 to day 4. Pictures taken with inverted microscope (scale bars=100 µm for magnification 4X, and 10X); B) Spheroids diameters (µm) over culture time represented as mean ± SD). C) Percentage of MTS and total protein of days 2 and 4 relative to day 1 of culture. (mean ± SEM, n=2-3). D) Cryosections stained with Hematoxylin & Eosin. Scale bar=100 µm. E) Cryosection immunolabeled with Ki-67(pink) and Dapi (blue). Major Figure scale bar= 100 µm. Minor Figure scale bar=20 µm.*

Phase contrast microscopy shows that at day 1, MDA-MB-231 cells inoculated at a cell density of 250.000 cells/mL, form small aggregates of approximately 90 µm diameter (Fig. 7 A and B). These aggregates further gathered, forming spheroids with increasing sizes and compactness over culture time. On average, spheroid diameters were 147 ± 64 µm (mean ± SD) at day 2 and 191 ± 95 µm (mean ± SD) at day 4 of culture (Fig. 7 B). From day 4 onwards the spheroids diameter was maintained (data not shown). To further monitor the morphology of the spheroids, histological analysis of spheroid cryosections were performed at day 4. H&E staining of sections revealed that spheroids were solid with cells homogeneously distributed and embedded in extracellular matrix presenting no evidence of necrotic cores (Fig. 7 D). Immunolabeling with the proliferative marker Ki-67 (Fig. 7 E) shows 15% proliferating cells, including cells within the spheroid. This proliferation percentage is in agreement with the observed 1.2-fold increase in total protein (Fig. 7 C). These results together with the MTS assay data (Fig. 7 C), show reduced proliferation in 3D cultures when compared with monolayer models, a pattern which has been broadly reported for many cancer cell lines including MDA-MB-231 [111, 113, 114]. Several factors, which induce this change in proliferation have been described, such as hypoxia and nutrients hindered diffusion, ECM elements and their stiffness [114–116]. Proliferation marker Ki-67 has been used as a prognostic marker for breast cancer, with most *in vivo* tumors having under 50% Ki-67$^+$cells. This contrasts with a very different percentage,100% Ki-67$^+$cells, reported in MDA-MB-231 monolayer [117].

Obtaining a realistic proliferation is vital for the assessment of potential chemotherapeutic agents, and also important for better understanding of breast cancer cell heterogeneity and classification. MDA-MB-231 cell line has been described as a highly proliferative triple-negative cells belonging to Basal-like tumors' type. Recently, a new subtype of breast tumors was identified, claudin-low [118]. These subtype is characterized for low or no expression of epithelial cell-cell adhesion molecules E-cadherin and Claudin-3,4 and 7 and high expression of EMT markers such as Vimentin and EMT transcription factors (e.g. Twist and Snail). The claudin-low subtype is also described to have a stemness signature by having high *CD44/CD24* and *CD49f/Epithelial cell adhesion molecule (EpCAM)* ratios, and by having a low percentage of Ki-67$^+$ cells, indicating lower proliferation when compared to other subtypes, such as Basal-like. A screening of several breast cancer cell lines identified nine cell lines, including MDA-MB-231, with the same expression profiles as claudin-low subtypes [119]. The main difference between cell lines and the primary tumor identified as claudin-low was the proliferation gene cluster, which could be a result of the selection imposed on cell lines or of the standard *in vitro* conditions. Thus, 3D models may give further insight about these cell lines by being able to reveal information that has been hiding under non-physiological culture conditions [120]. Moreover, MDA-MB-231 not expressing E-cadherin

could explain why these cells do not form spheroids spontaneously as they have their cell-cell-adhesion ability hampered. Hence, these cells require the addition of extrinsic ECM to form compact spheroids as they only tightly aggregate through integrin-β1 (cell-matrix interactions molecule) [99].

4.2. Cell Viability Assays

In order to rule out direct cytotoxic effects that could somehow conflict with migration assays, dose-response curves were performed to determine concentrations of the compounds [15]pyN_5, [16]pyN_5 and ARP-100, with no, or limited, effect on cells viability. The cytotoxicity activity of these compounds in both 2D and 3D models of MDA-MB-231 was assessed through MTS assay that detects viable and metabolic active cells. Since some of the cellular assays are performed in serum free conditions (e.g. scratch-assay), the cytotoxicity assays were also performed in serum-free conditions. Following the concentrations of ARP-100 used in literature [46,69], concentrations ranging 1-100 μM were chosen (Fig. 8). As for [15]pyN_5, [16]pyN_5 the same range of concentrations was adopted.

As depicted in Fig. 8 A and B, both pyridine containing macrocycles (py-macrocycles) induced a slight decrease on cell viability in 2D cultures at concentrations higher than 10 and 25 μM for [15]pyN_5 and [16]pyN_5, respectively. Up to 75 μM, viability was higher than 74%, decreasing to ~60% at 100 μM concentrations for both [15]pyN_5 and [16]pyN_5. The cytotoxicity profile observed in spheroids cultures was very similar between both py-macrocycles, with viability values never below 80% (Fig. 8 A and B).

Concentrations of ARP-100 up to 25 μM, showed no cytotoxicity in monolayers (Fig. 8 C). At a concentration of 50 μM, cell viability was 75% and decreased in a concentration dependent manner, attaining the value of 44% at 100 μM of ARP-100. In spheroid cultures, ARP-100 did not exhibit the same dose-response curve. Cell viability was never lower than 78%. In particular, for the ARP-100 concentrations of 75 and 100 μM, significantly higher ($p<0.05$ and $p<0.01$, respectively) cell viabilities were obtained in 3D cultures when compared to monolayer. These results suggest that the 3D model is more resistant to ARP-100 than the monolayer one. The toxicity mechanism for ARP-100 is not known and it is beyond our scope to explain the phenomenon in this specific case. Nevertheless, higher resistance of 3D models has been broadly reported [104, 108, 121], with the exception of some cell lines and drugs. As an example, it has been shown that in HT080 in 3D collagen fibers [121] and MCF-7 spheroids [94], proliferation and viability, respectively, were less affected by doxorubicin than monolayer cultures. The overall higher resistance of the 3D models has been related to the quiescence as aforementioned, ECM-mediated signaling pathways [122, 123] (e.g. apoptotic pathways) and even hypoxia-mediated P-glycoprotein up-expression [124]. Furthermore,

similarly to the gradient of nutrients and oxygen, drug penetration is also somewhat hindered in spheroids, once again mimicking the hindered diffusion in solid tumor [125, 126].

Following the viability assay studies, compounds' concentrations ranging 5-40 µM were adopted, in order to have a cell viability above 70 %.

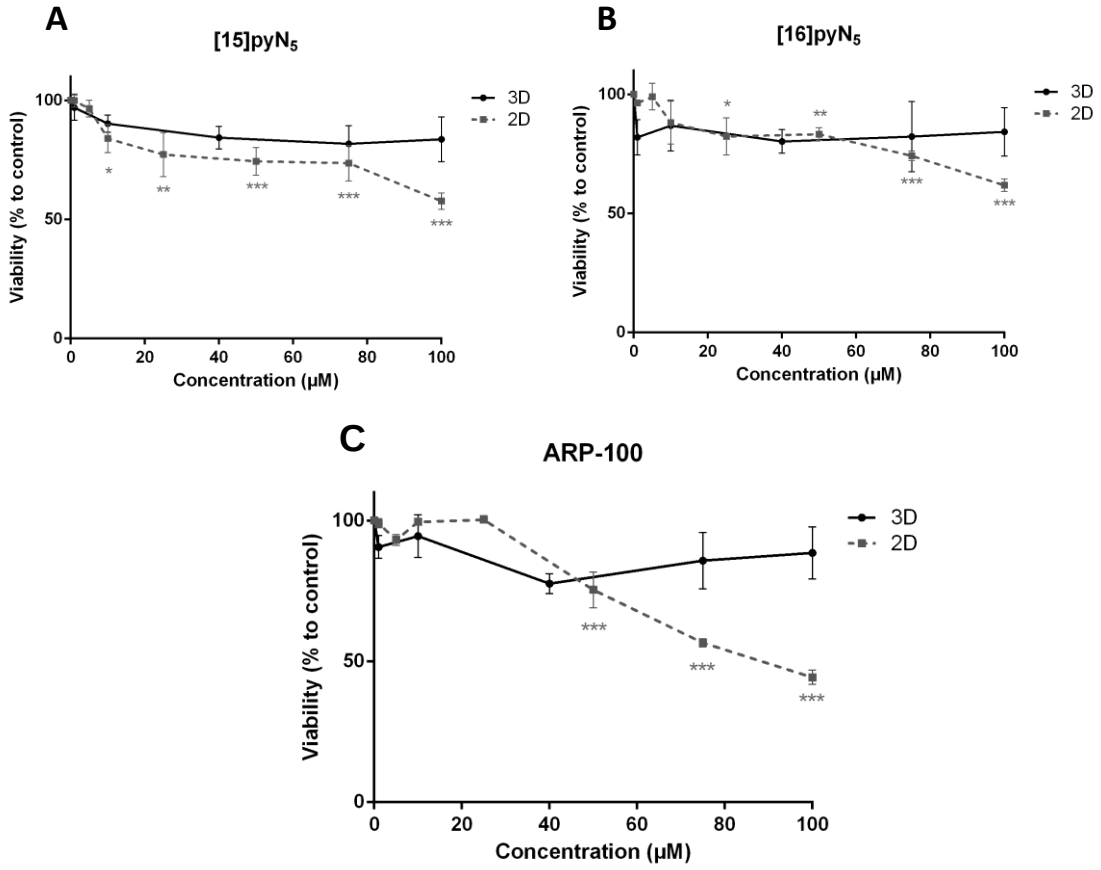

Figure 8. Effect of A) [15]pyN5, B) [16]pyN5 and C) ARP-100 on MDA-MB-231 cell viability on 2D and 3D models, evaluated through the MTS assay. *Results are expressed in percentage (mean± SEM, n=3;4) to respective controls, non-treated condition for [15]pyN$_5$ and [16]pyN$_5$ and 0.25% DMSO for ARP-100. Statistical significance is expressed relatively to respective controls as *p<0.05, **p<0.01, ***p<0.001.*

4.3.1. Optimization of Zymography technique and Media conditioning

A zymography technique, in which gelatin is used as substrate for MMP-2/9 and pro-MMP-2/9, was implemented to screen both enzyme activities. The first step is equivalent to a common SDS-PAGE, except for that it must be performed under non-reducing conditions. After electrophoresis, the gel is washed to remove SDS and then incubated with a buffer

containing MMP cofactors Ca^{2+} and Zn^{2+}, at a physiologic pH and salt concentration. In this last step, the MMPs contained in the gel degrade the gelatin, leaving a clear band after staining with Coomassie®. To confirm that the bands observed in the zymography gels were of MMP nature, gels developed in the presence or absence of EDTA (7.8 mM) were also compared. Indeed, EDTA inhibited the clear bands corresponding to the MMP-2 and MMP-9 molecular weights (Fig. 9 A).

Prior to medium conditioning, tests were performed to determine the optimal conditioning time (24, 48, 72 and 96 h) (Fig. 9 B), CM concentration and quantity of total protein of CM to be loaded in the gels. Moreover, culture volume was adjusted accordingly, in order to obtain a conditioning volume per cell in 3D cultures as in the two-dimensional system. The adopted ratio was of ~200,000 cells/mL Conditioning periods longer than 24 hours in serum free conditions resulted in increased cell death (30% cell death with 0.25% DMSO in a 48 h incubation) (data not shown), therefore it was established a conditioning incubation period not exceeding 24 hours. Furthermore, a volume concentration of ~100 X was adopted to ensure a sufficient gelatinase concentration.

Following this optimization, CM2D and CM3D were analyzed by zymography, showing a differential MMP-2 and 9 secretion (Fig. 9 C and D). Whereas in CM2D, there was more MMP-2 activity than MMP-9, in CM3D the contrary was observed. Therefore, culturing cells as spheroids induce different gelatinase secretion. The more *in vivo*-like cell-cell and cell-ECM interactions might have a role in this secretome change, as cell adhesion molecules such as integrins have been described to modulate MMPs expression [127, 128].

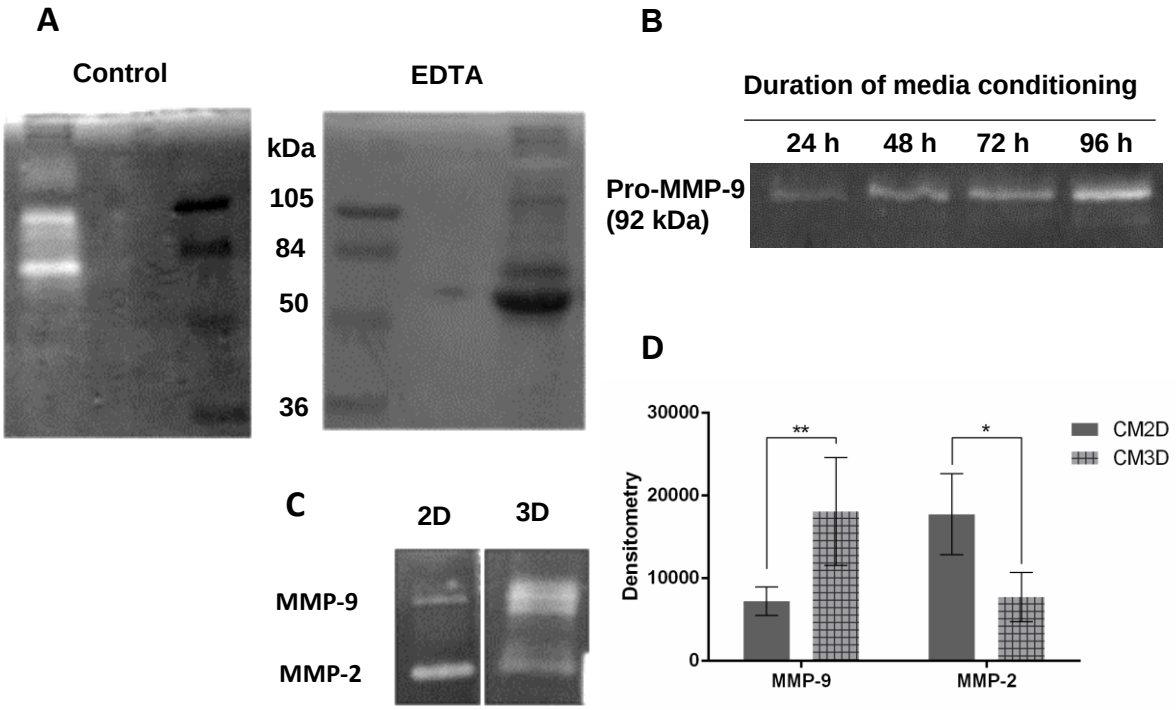

Figure 9. Gelatin Zymography Optimization. *A) Zymography gels incubated with and without 7.8 mM EDTA in the developing buffer. B) Medium conditioning duration (24-96 h) correlation with pro-MMP-9 secretion. C) Zymography gels with CM2D and CM3D.D) CM2D and CM3D (n=5) MMP-2 and MMP-9 gelatinolytic activity (arbitrary units of ImageJ software). Values are represented as mean ± SD, and statistical significance as *p<0.05 and ** p<0.01.*

4.3.2. Modified Zymography Assays for Gelatinolytic activity assessment

The objective of this work was to access possible direct MMP inhibitors. Since SDS has been indicated as a disrupting agent of TIMPs-MMP binding, the gelatinolytic activity that would be observed in the presence of SDS would be independent of the TIMP content [129]. Gelatinase inhibitors, similarly to TIMPs, might be released from the proteins in the SDS-PAGE gel [79]. Therefore, modifications were made to the zymography technique, as illustrated in Fig. 10. This technique differs from classical zymography by adding the compounds to the developing buffer incubation step, instead of incubating cells and their conditioned medium with the compounds. Therefore, changes in bands intensity directly reveal the influence that the compounds have in the MMP-2/9 gelatinolytic activity.

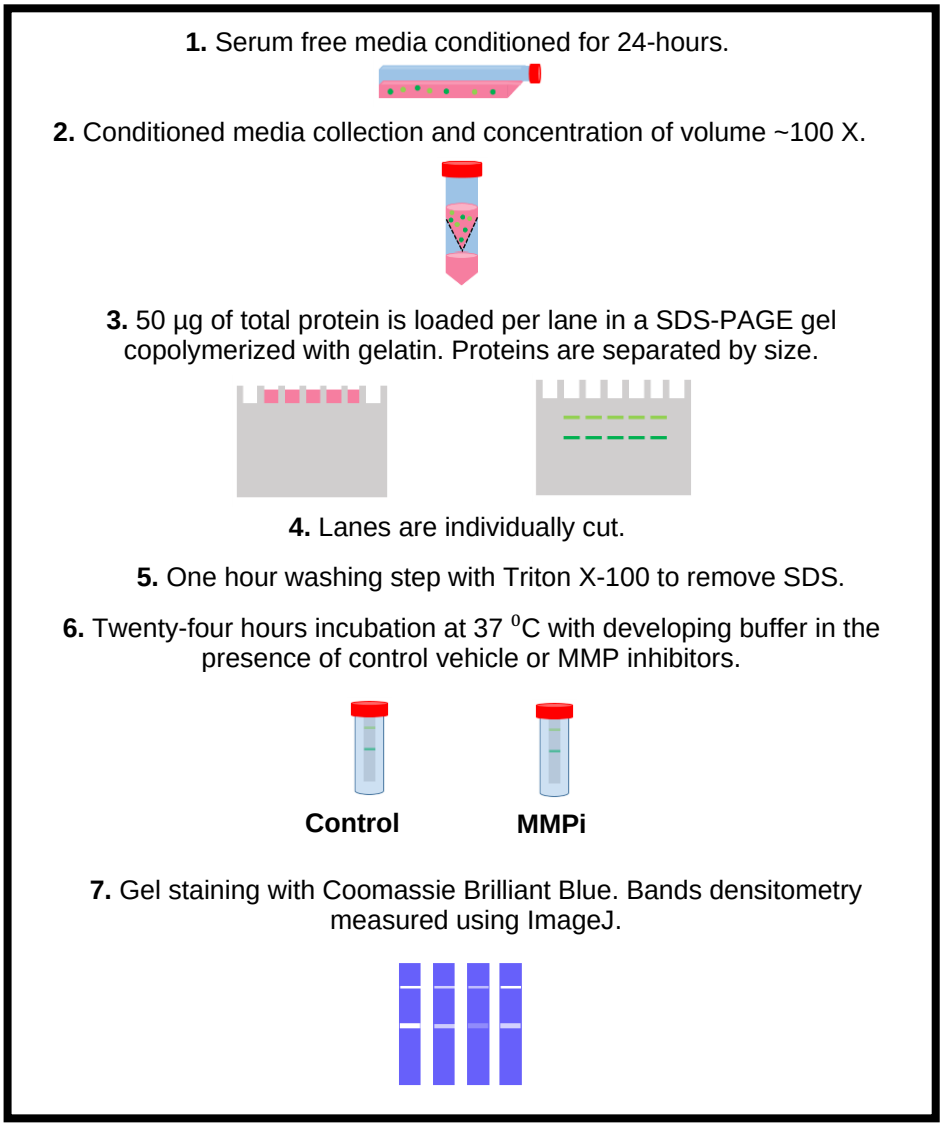

Figure 10. Schematic representation of the modified zymography technique adopted.

To analyze if the compounds [15]pyN$_5$, [16]pyN$_5$ and ARP-100 were able to inhibit MMP-2 and MMP-9 gelatinolytic activity in CM2D and CM3D, the modified zymography assay was performed (Fig. 11).

The method was shown to be reproducible, ie, gels (n=5) loaded with CM3D and treated with 5 and 10 µM of ARP-100, showed MMP-9/MMP-2 inhibition of 45±12%/58±12% (5 µM) and 56±14%/79±12% (10 µM), respectively (mean ± SD). Ten µM of ARP-100 tested in CM2D (Fig. 11 B) also inhibited more MMP-2 activity than MMMP-9. Hence, this differential inhibition may reflect the ARP-100 specificity for MMP-2. As seen in Fig. 11 A, for ARP-100 a ~100% Gelatinolytic activity (MMP2 and 9) inhibition was only observed at 40 µM.

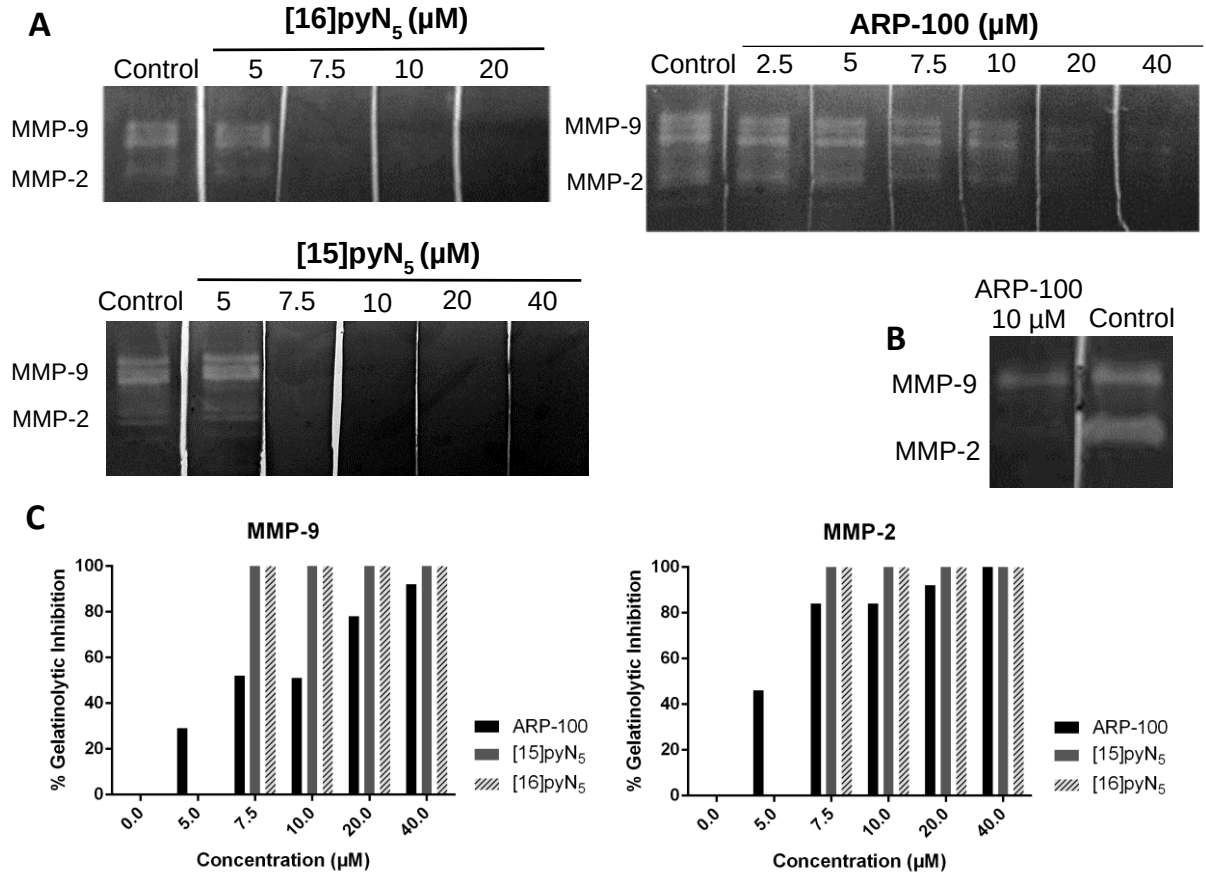

Figure 11. Effect of [16]pyN$_5$, [15]pyN$_5$ and ARP-100 on MMP2 and MMP-9 gelatinolytic activity. *A) CM3D zymography gels incubated with 5-40 μM of [16]pyN$_5$, [15]pyN$_5$ and ARP-100 in the developing buffer. B) CM2D zymography gels incubated with 10 μM of ARP-100 in the developing buffer. C) Gelatinolytic activity of MMP-2 and 9 from CM3D in the presence of [16]pyN$_5$, [15]pyN$_5$ and ARP-100, quantified through ImageJ software.*

The compounds [15]pyN$_5$ and [16]pyN$_5$ had the same inhibition profile, consisting in 100% inhibition for concentrations above 7.5 μM in CM3D (Fig. 11 A) and 10 μM in CM2D (data not shown), whereas no inhibition was obtained at 5 μM. The values of pZn^{2+} vs the concentration of [15]pyN$_5$ and [16]pyN$_5$, (Fig. 12) were simulated through Hyss program [130], using the compounds stability constants for Zn^{2+} and species distribution. The equivalence point obtained in the simulation coincided with the steep obtained in the zymography assay, pointing towards a correlation between the chelation of free Zn^{2+} and the inhibition of gelatinases by the compounds.

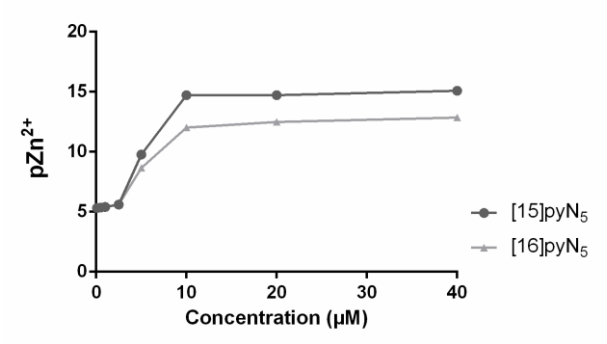

Figure 12. Values of pZn^{2+} (-log[Zn^{2+}]), calculated using* [130]*, for an aqueous solution of pH 7.4 containing Zn^{2+}(5 μM) and [16]pyN_5 and [15]pyN_5 (0.1-40 μM).

4.4. Migration Assays

In order to evaluate cell migration scratch and radial [96] assays were applied in 2D and 3D cultures, respectively. In monolayer cultures, scratch assays were performed in serum-free conditions, so that the closure of the scratch resulted for cells migration and not as a result of proliferation. In fact, significant effects for both py-macrocyles, when comparing to non-treated control condition, were observed for concentrations as low as 5 μM, with [16]pyN_5 and [15]pyN_5 decreasing cell migration 38 ± 2% and 21 ± 4%, respectively (Fig. 13). Py-macrocyles hampered migration also at higher concentrations, although no significant changes in the migration distance between the different concentrations tested, were observed. As for ARP-100, when compared to its control of 0.25% DMSO condition, although showing a slight inhibitor tendency, it was not found to be significant at any concentration tested. In fact, other mechanisms, besides MMP-2 and 9 inhibition, may be involved in these py-macrocycles hampering effect on monolayer cellular migration. Since MMP-2 and 9 inhibition is related to zinc chelation and MMPs have a highly conserved zinc-dependent catalytic site, [15]pyN_5 and [16]pyN_5 probably also inhibit other MMPs. Still, if py-macrocycles mechanism is based on overall MMPs inhibition, herein it is shown that although this inhibition affects cell migration on 2D culture conditions, it is not crucial. In fact, the essentiality of MMPs for invasion has been broadly describe, but its role in migration *per se* is still being disclosed.

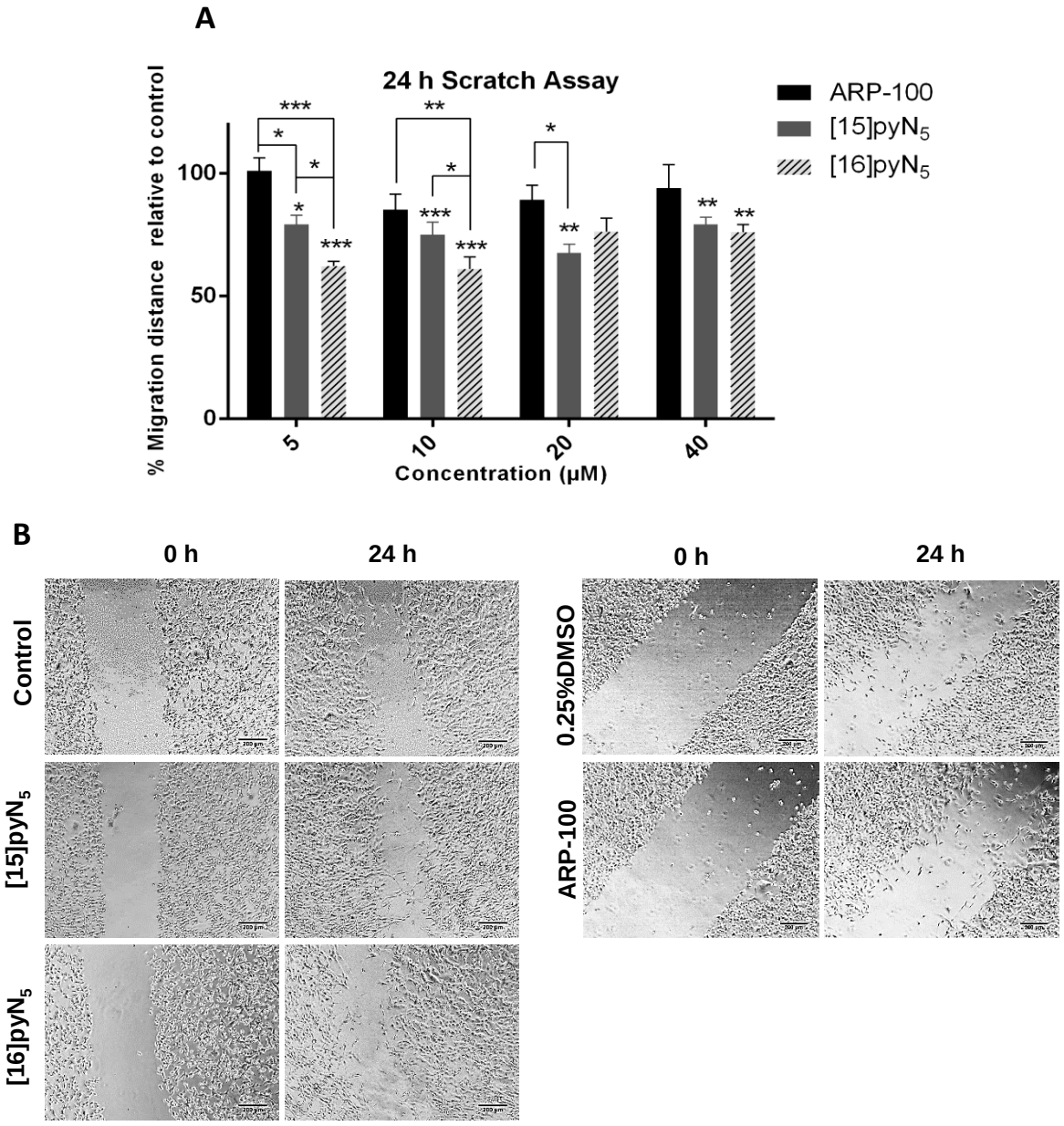

Figure 13. Scratch Assay with [15]pyN$_5$, [16]pyN$_5$ and ARP-100. A) *Cells migration represented as percentage (mean±SEM) relative to controls (non-treated condition for [15]pyN$_5$ and [16]pyN$_5$ and 0.25% DMSO for ARP-100), after 24 hours. B) Representative images of scratch assays at 0 and 24 hours with 5 μM of compounds and respective controls. Magnification 4 X, scale bar=200 μm. Statistical significance is represented as * p<0.05, ** p<0.01, *** p<0.001.*

Specifically in scratch assays, inhibition of MMPs through gene silencing [131, 132] antibody neutralization, [133] and pharmacological inhibitors such as batimastat [132] have in fact shown to have a deleterious effect on cell migration, although never ablating it completely. Since in scratch assay cell-matrix adhesions are not present, MMPs role in this motility is most probably by cleaving cell-attachment receptors directly, modulating cells adhesion during

migration [134] and triggering signaling pathways involved in migration and angiogenesis [40]. Indeed MT-MMP1 was shown to shed CD44 [135], MMP-9 to cleave CD44 and integrin $\alpha_M\beta2$ [136] and MMP-2 to cleave integrin αVβ3 [46], further promoting migration. Besides it is noteworthy that MMPs function extend beyond proteolytic functions, as their hemopexin domains have been shown to have important roles in migration [137, 138]. Dufour *et al* [139] showed that Gelatinases-induced migration did not depend on their proteolytic functions. MMP-9-induced migration shown to be dependent of its hinge and hemopexin domains and not to alter adhesion ability.

In the radial assays, 10% FBS supplemented medium was adopted, since serum-free medium disabled cells migration ability (data not shown). As depicted in Fig. 14, py-macrocycles showed a trend of decreased migration with increasing concentrations, being significant for 20 μM [16]pyN_5 which decreased cell migration 20±4%. ARP-100 only resulted in a significant cell migration decrease of 23±3% relative to control (0.25% DMSO) at 40 μM.

The results herein obtained in terms of MDA-MB-231 cellular migration under 3D and 2D conditions, suggest that spheroids are less susceptible than 2D models to the tested compounds. Several reasons may justify the observed effects. Although migrated distances in both 2D and 3D controls were similar (~260 μm), scratch assay was performed in serum free conditions while radial migration was performed with 10% FBS. Compounds bioavailability might be affected by FBS. ECM such as Matrigel™, which was present in the 3D culture both embedded in the spheroids and in the coating, has also been indicated to influence migration susceptibleness to compounds. Millerot-Serrurot *et al.* [140] described that HT1080 cells in 3D collagen I matrix had no significant migration inhibition, at the same doxorubicin concentrations that induced 70% inhibition in 2D models. Moreover, the GM6001 broad MMPi abrogates ovarian cancer cell lines monolayers and spheroids cell migration in collagen I matrix but not in Matrigel™, showing the relevance of ECM elements for migration and invasion [105]. Furthermore, as mentioned in the Chapter 4.2, similarly to *in vivo,* the compounds might not diffuse completely to the more central zone of the spheroid, affecting just the periphery.

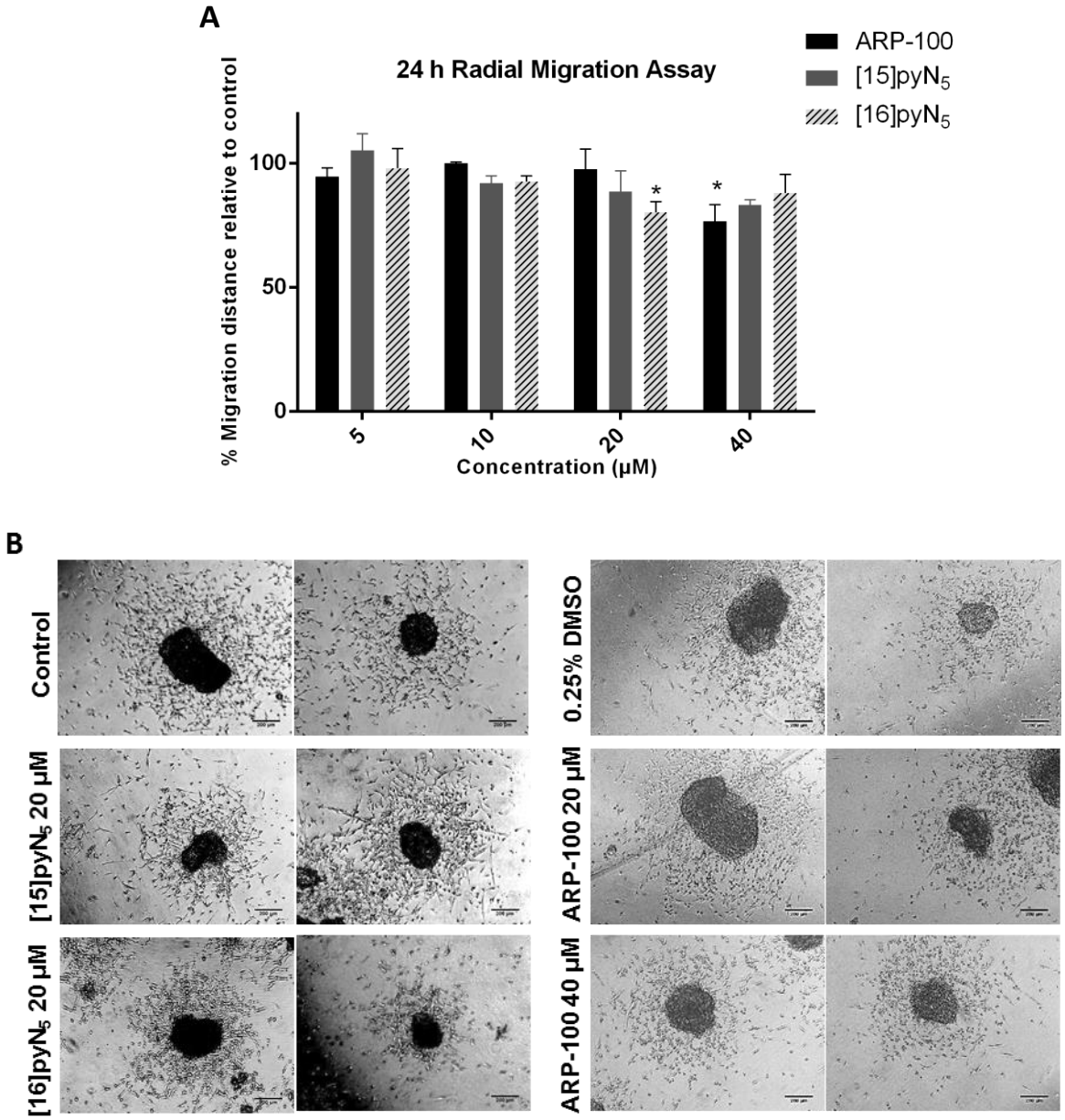

Figure 14. Radial migration assays with [15]pyN$_5$, [16]pyN$_5$ and ARP-100. A) *Cells migration represented as percentage (mean±SEM) relative to controls (non-treated condition for [15]pyN$_5$ and [16]pyN$_5$ and 0.25% DMSO for ARP-100), after 24 hours. B) Representative images of Radial Migration at 24 hours with compounds and respective controls. Magnification 4 X, scale bar=200 µm. Statistical significance is represented in * p<0.05 when compared to respective controls.*

5. Conclusion

In this work, 3D models of human breast cancer cells (MDA-MB-231 cells) were successfully implemented and characterized. These models present important differences relatively to monolayers, in terms of ECM presence and cell organization inducing different proliferation profile and gelatinases activity. These differences may justify the different susceptibility of the model to the compounds herein tested as possible anti-migratory agents.

The two macrocyclic compounds containing pyridine reduced cell migration in 2D models, and [16]pyN_5 in 3D models, probably involving MMP-2 and 9, or even overall MMPs proteolytic activity inhibition. To further clarify both, the mechanism of these compounds and the roles of MMPs, the next step of this study will be to perform invasion assays and eventually analyze if the py-macrocycles induce changes in EMT related pathways such as PI3K.

If [15]pyN_5 and [16]pyN_5 prove to be efficient inhibitors of other metastization hallmarks, they might be a good starting point for new molecules design. Molecular Docking analysis would have to be performed to understand the interaction of these compounds with the MMPs, and consequently their inhibition mechanism. Although these py-macrocycles zinc binding ability was enough for 100% inhibition of gelatinases activity, specificity for zinc over other essential divalent cations is highly desirable [31]. Moreover, although specificity of MMPs over other proteins is much desired, ARP-100 not surpassing the py-macrocycles effects, raises doubts about the value of selectivity within the MMPs group.

If 3D models keep their relative insensibility to compounds in invasion assays, the results should not be perceived with less interest. As mentioned in the introduction, 3D models came to bridge the more complex models with monolayers to prevent drug attrition. Meaning that compounds that usually fail in latter phases of drug development, might fail earlier by testing them in these 3D models. And so the model might be in fact fulfilling its original scope. Besides, the 3D models have a great potential of giving further insights on tumors progression and hence better strategies to target them.

4. References

[1] J. Ferlay, I. Soerjomataram, M. Ervik, R. Dikshit, S. Eser, C. Mathers, M. Rebelo, D. Parkin, D. Forman, and F. Bray, “Cancer Incidence and Mortality Worldwide: IARC CancerBase,” *GLOBOCAN 2012 v1.0*, vol. 11, 2013.

[2] N. Howlader, A. Noone, M. Krapcho, J. Garshell, D. Miller, S. Altekruse, C. Kosary, M. Yu, J. Ruhl, Z. Tatalovich, A. Mariotto, D. Lewis, H. Chen, E. Feuer, and C. KA, “SEER Cancer Statistics Review, 1975-2012,” *National Cancer Institute. Bethesda, MD*, 2015. [Online]. Available: http://seer.cancer.gov/csr/1975_2012/. [Accessed: 20-Mar-2016].

[3] P. Friedl and K. Wolf, “Tumour-cell invasion and migration: diversity and escape mechanisms.,” *Nat. Rev. Cancer*, vol. 3, no. 5, pp. 362–74, May 2003.

[4] M. Egeblad and Z. Werb, “New functions for the matrix metalloproteinases in cancer progression.,” *Nat. Rev. Cancer*, vol. 2, no. 3, pp. 161–74, Mar. 2002.

[5] R. C. S. Figueira, L. R. Gomes, J. S. Neto, F. C. Silva, I. D. C. G. Silva, and M. C. Sogayar, “Correlation between MMPs and their inhibitors in breast cancer tumor tissue specimens and in cell lines with different metastatic potential.,” *BMC Cancer*, vol. 9, no. 20, 2009.

[6] B. Fingleton, “MMPs as therapeutic targets-still a viable option?,” *Semin Cell Dev Biol*, vol. 19, no. 1, pp. 61–68, 2008.

[7] I. Kola and J. Landis, “Can the pharmaceutical industry reduce attrition rates?,” *Nat. Rev. Drug Discov.*, vol. 3, no. August, pp. 1–5, 2004.

[8] J. A. Hickman, R. Graeser, R. de Hoogt, S. Vidic, C. Brito, M. Gutekunst, H. van der Kuip, and IMI PREDECT consortium, “Three-dimensional models of cancer for pharmacology and cancer cell biology: Capturing tumor complexity in vitro/ex vivo,” *Biotechnol. J.*, vol. 9, no. 9, pp. 1115–1128, 2014.

[9] R. Lin and H. Chang, “Recent advances in three-dimensional multicellular spheroid culture for biomedical research,” *Biotechnol. J.*, pp. 1172–1184, 2008.

[10] A. Jemal, M. M. Center, C. DeSantis, and E. M. Ward, “Global patterns of cancer incidence and mortality rates and trends.,” *Cancer Epidemiol. Biomarkers Prev.*, vol. 19, no. 8, pp. 1893–907, Aug. 2010.

[11] B. Weigelt, J. L. Peterse, and L. J. van ’t Veer, “Breast cancer metastasis: markers and models.,” *Nat. Rev. Cancer*, vol. 5, no. 8, pp. 591–602, Aug. 2005.

[12] D. Lauffenburger and H. F, “Cell migration: a physically integrated molecular process.,” *Cell*, vol. 84, no. 3, pp. 359–69, Feb. 1996.

[13] T. T. Onder, P. B. Gupta, S. A. Mani, J. Yang, E. S. Lander, and R. A. Weinberg, “Loss of E-Cadherin Promotes Metastasis via Multiple Downstream Transcriptional Pathways,” *Cancer Res.*, vol. 68, no. 10, pp. 3645–3654, 2008.

[14] K. Polyak and R. A. Weinberg, “Transitions between epithelial and mesenchymal states: acquisition of malignant and stem cell traits,” *Nat. Rev. Cancer*, vol. 9, no. 4, pp. 265–273, 2009.

[15] A. M. Shannon, D. J. Bouchier-Hayes, C. M. Condron, and D. Toomey, “Tumour hypoxia, chemotherapeutic resistance and hypoxia-related therapies,” *Cancer Treat. Rev.*, vol. 29, no. 4, pp. 297–307, 2003.

[16] K. R. Levental, H. Yu, L. Kass, J. N. Lakins, J. T. Erler, S. F. T. Fong, K. Csiszar, A. Giaccia, M. Yamauchi, D. L. Gasser, and V. M. Weaver, “Matrix Crosslinking Forces Tumor Progression by Enhancing Integrin signaling,” *Cell*, vol. 139, no. 5, pp. 891–906, 2009.

[17] L.-M. Postovit, D. E. Abbott, S. L. Payne, W. W. Wheaton, N. V Margaryan, R. Sullivan, M. K. Jansen, K. Csiszar, M. J. C. Hendrix, and D. A. Kirschmann, “Hypoxia/reoxygenation: a dynamic regulator of lysyl oxidase-facilitated breast cancer migration.,” *J. Cell. Biochem.*, vol. 103, no. 5, pp. 1369–78, 2008.

[18] W. Li and Y. Kang, “Probing the Fifty Shades of EMT in Metastasis,” *Trends in Cancer*, vol. 2, no. 2, pp. 65–67, 2016.

[19] K. Wolf, I. Mazo, H. Leung, K. Engelke, U. H. von Andrian, E. I. Deryugina, A. Y. Strongin, E.-B. Bröcker, and P. Friedl, “Compensation mechanism in tumor cell migration: mesenchymal-amoeboid transition after blocking of pericellular proteolysis.,” *J. Cell Biol.*, vol. 160, no. 2, pp. 267–77, Jan. 2003.

[20] A. Köhrmann, U. Kammerer, M. Kapp, J. Dietl, and J. Anacker, “Expression of matrix metalloproteinases (MMPs) in primary human breast cancer and breast cancer cell lines: New findings and review of the literature.,” *BMC Cancer*, vol. 9, p. 188, Jan. 2009.

[21] R. Roy, J. Yang, and M. Moses, “Matrix metalloproteinases as novel biomarkers and potential therapeutic targets in human cancer.,” *J. Clin. Oncol.*, vol. 27, no. 31, pp. 5287–97, Nov. 2009.

[22] W. Bode, C. Fernandez-Catalan, H. Tschesche, F. Grams, H. Nagase, and K. Maskos, “Structural properties of matrix metalloproteinases.,” *Cell. Mol. Life Sci.*, vol. 55, no. 4, pp. 639–652, 1999.

[23] A. K. Chaudhary, S. Pandya, K. Ghosh, and A. Nadkarni, “Matrix metalloproteinase and its drug targets therapy in solid and hematological malignancies: an overview.,” *Mutat. Res.*, vol. 753, no. 1, pp. 7–23, 2013.

[24] J. Zhu, G. Xiong, C. Trinkle, and R. Xu, “Integrated extracellular matrix signaling in mammary gland development and breast cancer progression.,” *Histol. Histopathol.*, 2014.

[25] C. Streuli, “Extracellular matrix remodelling and cellular differentiation.,” *Curr. Opin. Cell Biol.*, vol. 11, no. 5, pp. 634–40, Oct. 1999.

[26] K. Kessenbrock, V. Plaks, and Z. Werb, “Matrix metalloproteinases: regulators of the tumor microenvironment.,” *Cell*, vol. 141, no. 1, pp. 52–67, Apr. 2010.

[27] K. J. Davies, “The Complex Interaction of Matrix Metalloproteinases in the Migration of Cancer Cells through Breast Tissue Stroma.,” *Int. J. Breast Cancer*, vol. 2014, Jan. 2014.

[28] H. Nagase and J. F. Woessner, “Matrix metalloproteinases.,” *J. Biol. Chem.*, vol. 274, no. 31, pp. 21491–21494, 1999.

[29] L. Aureli, M. Gioia, I. Cerbara, S. Monaco, G. Fasciglione, S. Marini, P. Ascenzi, A. Topai, and M. Coletta, “Structural Bases for Substrate and Inhibitor Recognition by Matrix Metalloproteinases,” *Curr. Med. Chem.*, vol. 15, no. 22, pp. 2192–2222, 2008.

[30] R. K. Harrison, B. Chang, L. Niedzwiecki, and R. L. Stein, “Mechanistic studies on the human matrix metalloproteinase stromelysin.,” *Biochemistry*, vol. 31, pp. 10757–10762, 1992.

[31] J. a. Jacobsen, J. L. Major Jourden, M. T. Miller, and S. M. Cohen, “To bind zinc or not to bind zinc: An examination of innovative approaches to improved metalloproteinase inhibition,” *Biochim. Biophys. Acta - Mol. Cell Res.*, vol. 1803, no. 1, pp. 72–94, 2010.

[32] K. Brew and H. Nagase, “The tissue inhibitors of metalloproteinases (TIMPs): an ancient family with structural and functional diversity,” *Biochim. Biophys. Acta*, vol. 1803, no. 1, pp. 55–71, 2010.

[33] W. G. Stetler-Stevenson, “Tissue Inhibitors of Metalloproteinases in cell signaling,” *Sci Signal*, vol. 1, no. 27, 2008.

[34] S. Leppa, T. Saarto, L. Vehmanen, C. Blomqvist, and I. Elomaa, “A high serum matrix metalloproteinase-2 level is associated with an adverse prognosis in node-positive breast carcinoma,” *Clin Cancer Res*, vol. 10, no. 3, pp. 1057–1063, 2004.

[35] H.-C. Li, D.-C. Cao, Y. Liu, Y.-F. Hou, J. Wu, J.-S. Lu, G.-H. Di, G. Liu, F.-M. Li, Z.-L. Ou, C. Jie, Z.-Z. Shen, and Z.-M. Shao, “Prognostic value of matrix metalloproteinases (MMP-2 and MMP-9) in patients with lymph node-negative breast carcinoma.,” *Breast Cancer Res. Treat.*, vol. 88, no. 1, pp. 75–85, 2004.

[36] S. Ranuncolo, E. Matos, D. Loria, and M. Vilensky, “Circulating 92-kilodalton matrix metalloproteinase (MMP-9) activity is enhanced in the euglobulin plasma fraction of head and neck squamous cell carcinoma,” *Cancer*, pp. 201–204, 2002.

[37] S. Saad, D. J. Gottlieb, K. F. Bradstock, C. M. Overall, and L. J. Bendall, “Cancer cell-associated fibronectin induces release of matrix metalloproteinase-2 from normal fibroblasts,” *Cancer Res.*, vol. 62, no. 18, pp. 283–289, 2002.

[38] V. C. Ardi, P. E. Van den Steen, G. Opdenakker, B. Schweighofer, E. I. Deryugina, and J. P. Quigley, “Neutrophil MMP-9 proenzyme, unencumbered by TIMP-1, undergoes efficient activation in vivo and catalytically induces angiogenesis via a basic fibroblast growth factor (FGF-2)/FGFR-2 pathway,” *J Biol Chem*, vol. 284, no. 38, pp. 25854–25866, 2009.

[39] A. Jezierska and T. Motyl, “Matrix metalloproteinase-2 involvement in breast cancer progression: a mini-review.,” *Med. Sci. Monit.*, vol. 15, no. 2, pp. RA32–40, Feb. 2009.

[40] B. Bauvois, “New facets of matrix metalloproteinases MMP-2 and MMP-9 as cell surface transducers: Outside-in signaling and relationship to tumor progression,” *Biochim. Biophys. Acta - Rev. Cancer*, vol. 1825, no. 1, pp. 29–36, 2012.

[41] A. Dufour, S. Zucker, N. S. Sampson, C. Kuscu, and J. Cao, “Role of Matrix Metalloproteinase-9 Dimers in Cell Migration: Design of inhibitory peptides,” *J. Biol. Chem.*, vol. 285, no. 46, pp. 35944–35956, 2010.

[42] S. L. Dallas, J. L. Rosser, G. R. Mundy, and L. F. Bonewald, “Proteolysis of Latent Transforming Growth Factor-β (TGF-β)-binding Protein-1 by Osteoclasts: a cellular mechanism for release of TGF-β from bone matrix,” *J. Biol. Chem.*, vol. 277, no. 24, pp. 21352–21360, 2002.

[43] Q. Yu and I. Stamenkovic, “Cell surface-localized metalloproteinase-9 proteolyically activates TGF-beta and promotes tumour invasion and angiogenesis,” *Genes Dev.*, vol. 14, pp. 163–176, 2000.

[44] J. Massagué, “TGFβ in cancer,” *Cell*, vol. 134, no. 2, pp. 215–230, 2008.

[45] G. Bergers, R. Brekken, G. Mcmahon, T. H. Vu, T. Itoh, K. Tamaki, K. Tanzawa, P. Thorpe, S. Itohara, and D. Hanahan, “Matrix metalloproteinase-9 triggers the angiogenic switch during carcinogenesis,” *Nat. Cell Biol.*, vol. 2, no. 10, pp. 737–744, 2000.

[46] C. Chetty and S. Lakka, “MMP-2 alters VEGF expression via αVβ3 integrin-mediated PI3K/AKT signaling in A549 lung cancer cells,” *Int. J. Cancer*, vol. 127, no. 5, pp. 1081–1095, 2010.

[47] E. S. Nakamura, K. Koizumi, M. Kobayashi, and I. Saiki, “Inhibition of

lymphangiogenesis-related properties of murine lymphatic endothelial cells and lymph node metastasis of lung cancer by the matrix metalloproteinase inhibitor MMI270," *Cancer Sci*, vol. 95, no. 1, pp. 25–31, 2004.

[48] K. D. C. Dahl, J. Symowicz, Y. Ning, E. Gutierrez, D. A. Fishman3, B. P. Adley, M. S. Stack, and L. G. Hudson, "Matrix metalloproteinase (MMP)-9 is a mediator of epidermal growth factor dependent E-cadherin loss in ovarian carcinoma cells," *Cancer Res.*, vol. 68, no. 12, pp. 4606–4613, 2008.

[49] B. J. Ahn, H. Le, M. W. Shin, S.-J. Bae, E. J. Lee, H.-J. Wee, J. H. Cha, J.-H. Park, H. S. Lee, H.-J. Lee, H. Jung, Z.-Y. Park, S. H. Park, B. W. Han, J. H. Seo, E. H. Lo, and K.-W. Kima, "The N-terminal ectodomain of Ninjurin1 liberated by MMP9 has chemotactic activity," *Biochem. Biophys. Res. Commun.*, vol. 428, no. 4, pp. 438–444, 2012.

[50] G. Giannelli, J. Falk-Marzillier, O. Schiraldi, W. G. Stetler-Stevenson, and V. Quaranta, "Induction of cell migration by matrix metalloprotease-2 cleavage of laminin-5.," *Science*, vol. 277, no. 5323, pp. 225–228, 1997.

[51] B. C. Patterson and Q. A. Sang, "Angiostatin-converting enzyme activities of human matrilysin (MMP-7) and gelatinase B/type IV collagenase (MMP-9)," *J Biol Chem*, vol. 272, no. 46, pp. 28823–28825, 1997.

[52] Y. Hamano, M. Zeisberg, H. Sugimoto, J. C. Lively, Y. Maeshima, C. Yang, R. O. Hynes, Z. Werb, A. Sudhakar, and R. Kalluri, "Physiological levels of tumstatin, a fragment of collagen IV α3 chain, are generated by MMP-9 proteolysis and suppress angiogenesis via αVβ3 integrin," *Cancer Cell*, vol. 3, no. 6, pp. 589–601, 2003.

[53] K. S. Leifler, S. Svensson, A. Abrahamsson, C. Bendrik, J. Robertson, J. Gauldie, A.-K. Olsson, and C. Dabrosin, "Inflammation Induced by MMP-9 Enhances Tumor Regression of Experimental Breast Cancer," *J. Immunol.*, vol. 190, no. 8, pp. 4420–4430, 2013.

[54] M. R. Acharya, J. Venitz, W. D. Figg, and A. Sparreboom, "Chemically modified tetracyclines as inhibitors of matrix metalloproteinases.," *Drug Resist. Updat.*, vol. 7, no. 3, pp. 195–208, Jun. 2004.

[55] B. G. Rao, "Recent developments in the design of specific Matrix Metalloproteinase inhibitors aided by structural and computational studies.," *Curr. Pharm. Des.*, vol. 11, no. 3, pp. 295–322, 2005.

[56] V. M. Macaulay, K. J. O'Byrne, M. P. Saunders, J. P. Braybrooke, L. Long, F. Gleeson, C. S. Mason, A. L. Harris, P. Brown, and D. C. Talbot, "Phase I study of intrapleural batimastat (BB-94), a matrix metalloproteinase inhibitor, in the treatment of malignant pleural effusions.," *Clin. Cancer Res.*, vol. 5, no. 3, pp. 513–520, 1999.

[57] M. Hidalgo and S. G. Eckhardt, "Development of matrix metalloproteinase inhibitors in

cancer therapy.," *J. Natl. Cancer Inst.*, vol. 93, no. 3, pp. 178–193, 2001.

[58] S. Wojtowicz-praga, "Clinical Potential of Matrix Metalloprotease inhibitors," *Expert Opin. Ther. Pat.*, vol. 1, no. 2, pp. 117–129, 1999.

[59] J. a. Sparano, P. Bernardo, P. Stephenson, W. J. Gradishar, J. N. Ingle, S. Zucker, and N. E. Davidson, "Randomized phase III trial of marimastat versus placebo in patients with metastatic breast cancer who have responding or stable disease after first-line chemotherapy: Eastern Cooperative Oncology Group trial E2196.," *J. Clin. Oncol.*, vol. 22, no. 23, pp. 4683–4690, 2004.

[60] D. Bissett, K. J. O'byrne, P. J. Von, U. Gatzemeier, A. Price, M. Nicolson, R. Mercier, E. Mazabel, C. Penning, M. H. Zhang, F. A. Shepherd, and M. A. Collier, "Phase III Study of Matrix Metalloproteinase Inhibitor Prinomastat in Non-Small-Cell Lung Cancer," *J. Clin. Oncol.*, vol. 23, no. 4, pp. 842–849, 2005.

[61] R. Renkiewicz, L. Qiu, C. Lesch, X. Sun, R. Devalaraja, T. Cody, E. Kaldjian, H. Welgus, and V. Baragi, "Broad-spectrum matrix metalloproteinase inhibitor marimastat-induced musculoskeletal side effects in rats.," *Arthritis Rheum.*, vol. 48, no. 6, pp. 1742–9, 2003.

[62] J. F. Fisher and S. Mobashery, "Recent advances in MMP inhibitor design," *Cancer Metastasis Rev.*, vol. 25, no. 1, pp. 115–136, 2006.

[63] S. Brown, M. M. Bernardo, Z. Li, L. P. Kotra, Y. Tanaka, and R. Fridman, "Potent and Selective Mechanism-Based Inhibition of Gelatinases," vol. 122, pp. 6799–6800, 2000.

[64] O. Kleifeld, L. P. Kotra, D. C. Gervasi, S. Brown, M. M. Bernardo, R. Fridman, S. Mobashery, and I. Sagi, "X-ray absorption studies of human matrix metalloproteinase-2 (MMP-2) bound to a highly selective mechanism-based inhibitor. comparison with the latent and active forms of the enzyme.," *J. Biol. Chem.*, vol. 276, no. 20, pp. 17125–31, May 2001.

[65] M. M. Aye, C. Ma, H. Lin, K. a Bower, R. C. Wiggins, and J. Luo, "Ethanol-induced in vitro invasion of breast cancer cells: the contribution of MMP-2 by fibroblasts.," *Int. J. Cancer*, vol. 112, no. 5, pp. 738–46, Dec. 2004.

[66] A. Krüger, M. J. E. Arlt, M. Gerg, C. Kopitz, M. M. Bernardo, M. Chang, S. Mobashery, and R. Fridman, "Antimetastatic activity of a novel mechanism-based gelatinase inhibitor.," *Cancer Res.*, vol. 65, no. 9, pp. 3523–6, May 2005.

[67] A. Rossello, E. Nuti, E. Orlandini, P. Carelli, S. Rapposelli, M. Macchia, F. Minutolo, L. Carbonaro, A. Albini, R. Benelli, G. Cercignani, G. Murphy, and A. Balsamo, "New N-arylsulfonyl-N-alkoxyaminoacetohydroxamic acids as selective inhibitors of gelatinase A (MMP-2).," *Bioorg. Med. Chem.*, vol. 12, no. 9, pp. 2441–50, May 2004.

[68] T. Tuccinardi, A. Martinelli, E. Nuti, P. Carelli, F. Balzano, G. Uccello-Barretta, G.

Murphy, and A. Rossello, “Amber force field implementation, molecular modelling study, synthesis and MMP-1/MMP-2 inhibition profile of (R)- and (S)-N-hydroxy-2-(N-isopropoxybiphenyl-4-ylsulfonamido)-3-methylbutanamides.,” *Bioorg. Med. Chem.*, vol. 14, no. 12, pp. 4260–76, Jun. 2006.

[69] J. Cai, H. Tang, L. Xu, X. Wang, C. Yang, S. Ruan, J. Guo, S. Hu, and Z. Wang, “Fibroblasts in omentum activated by tumor cells promote ovarian cancer growth, adhesion and invasiveness,” *Carcinogenesis*, vol. 33, no. 1, pp. 20–29, 2012.

[70] S. Boissier, M. Ferreras, O. Peyruchaud, S. Magnetto, F. H. Ebetino, M. Colombel, P. Delmas, J. Delaisse, and P. Cle, “Bisphosphonates Inhibit Breast and Prostate Carcinoma Cell Invasion , an Early Event in the Formation of Bone Metastases Bisphosphonates Inhibit Breast and Prostate Carcinoma Cell Invasion , an Early Event in the Formation of Bone Metastases 1,” *Cancer Res.*, vol. 60, pp. 2949–2954, 2000.

[71] S.-G. Shian, Y.-R. Kao, F. Y.-H. Wu, and C.-W. Wu, “Inhibition of invasion and angiogenesis by zinc-chelating agent disulfiram.,” *Mol. Pharmacol.*, vol. 64, no. 5, pp. 1076–84, Nov. 2003.

[72] G. Y. Liu, N. Frank, H. Bartsch, and J. K. Lin, “Induction of apoptosis by thiuramdisulfides, the reactive metabolites of dithiocarbamates, through coordinative modulation of NFκB, c-fos/c-jun, and p53 proteins,” *Mol. Carcinog.*, vol. 22, no. 4, pp. 235–246, 1998.

[73] Z. K. Hassan and M. H. Daghestani, “Curcumin effect on MMPs and TIMPs genes in a breast cancer cell line.,” *Asian Pac. J. Cancer Prev.*, vol. 13, no. 7, pp. 3259–64, Jan. 2012.

[74] G. Batist, F. Patenaude, P. Champagne, D. Croteau, C. Levinton, C. Hariton, B. Escudier, and E. Dupont, “Neovastat (Ae-941) in refractory renal cell carcinoma patients: report of a phase II trial with two dose levels,” *Ann. Oncol.*, vol. 13, no. 8, pp. 1259–1263, Aug. 2002.

[75] C. L. Loprinzi, R. Levitt, D. L. Barton, J. a Sloan, P. J. Atherton, D. J. Smith, S. R. Dakhil, D. F. Moore, J. E. Krook, K. M. Rowland, M. a Mazurczak, A. R. Berg, and G. P. Kim, “Evaluation of shark cartilage in patients with advanced cancer: a North Central Cancer Treatment Group trial.,” *Cancer*, vol. 104, no. 1, pp. 176–82, Jul. 2005.

[76] L. M. Golub, J. M. Goodson, H. M. Lee, A. M. Vidal, T. F. Mcnamara, and N. S. Ramamurthy, “Tetracyclines Inhibit Tissue Collagenases : Effects of Ingested Low-Dose and Local Delivery Systems,” *J. Periodontol.*, vol. 56, no. 11, pp. 93–97, 1985.

[77] L. M. Golub, T. F. McNamara, G. D’Angelo, R. a Greenwald, and N. S. Ramamurthy, “A non-antibacterial chemically-modified tetracycline inhibits mammalian collagenase activity.,” *J. Dent. Res.*, vol. 66, no. 8, pp. 1310–1314, 1987.

[78] Y. Gu, H.-M. Lee, L. M. Golub, T. Sorsa, Y. T. Konttinen, and S. R. Simon, “Inhibition

of breast cancer cell extracellular matrix degradative activity by chemically modified tetracyclines.," *Ann. Med.*, vol. 37, no. 6, pp. 450–60, Jan. 2005.

[79] B. L. Lokeshwar, M. G. Selzer, B. Q. Zhu, N. L. Block, and L. M. Golub, "Inhibition of cell proliferation, invasion, tumor growth and metastasis by an oral non-antimicrobial tetracycline analog (COL-3) in a metastatic prostate cancer model," *Int. J. Cancer*, vol. 98, no. 2, pp. 297–309, 2002.

[80] R. Seftor and E. Seftor, "Chemically Modified Tetracyclines: Inhibition of Laminin 5 γ2 Chain Promigratory Fragments and Vasculogenic Mimicry 1 Supported by NIH/National Cancer Institute," *Mol. Cancer Ther.*, vol. 1, pp. 1173–1179, 2002.

[81] B. L. Lokeshwar, H. L. Houston-Clark, M. G. Selzer, N. L. Block, and L. M. Golub, "Potential Application of a Chemically Modified Non-Antimicrobial Tetracycline (CMT-3) Against Metastatic Prostate Cancer," *Adv. Dent. Res.*, vol. 12, no. 1, pp. 97–102, 1998.

[82] L. M. Coussens, B. Fingleton, and L. M. Matrisian, "Matrix metalloproteinase inhibitors and cancer: trials and tribulations.," *Science*, vol. 295, no. 5564, pp. 2387–2392, 2002.

[83] S. A. Eccles, G. M. Box, W. J. Court, E. A. Bone, W. Thomas, and P. D. Brown, "Control of Lymphatic and Hematogenous Metastasis of a Rat Mammary Carcinoma by the Matrix Metalloproteinas Inhibitor Control of Lymphatic and Hematogenous Metastasis of a Rat Mammary Carcinoma," *Cancer Res.*, vol. 56, pp. 2815–2822, 1996.

[84] R. D. Hancock, "Chelate ring size and metal ion selection. The basis of selectivity for metal ions in open-chain ligands and macrocycles," *J. Chem. Educ.*, vol. 69, no. 8, pp. 615–621, 1992.

[85] E. Kimura, S. Aoki, E. Kikuta, and T. Koike, "A macrocyclic zinc(II) fluorophore as a detector of apoptosis.," *Proc. Natl. Acad. Sci. U. S. A.*, vol. 100, no. 7, pp. 3731–3736, 2003.

[86] F. E. Jacobsen, J. a. Lewis, and S. M. Cohen, "A new role for old ligands: Discerning chelators for zinc metalloproteinases," *J. Am. Chem. Soc.*, vol. 128, no. 10, pp. 3156–3157, 2006.

[87] Yu. M, Lim. N H, Ellis. S, Nagase. H, Triccas, J, Rutledge. P J. Todd, M H., Incorporation of Bulky and Cationic Cyclam-Triazole Moieties into Marimastat Can Generate Potent MMP Inhibitory Activity without Inducing Cytotoxicity, *ChemistryOpen*, vol 2, pp. 99-105

[88] A. S. Fernandes, M. F. Cabral, J. Costa, M. Castro, R. Delgado, M. G. B. Drew, and V. Félix, "Two macrocyclic pentaaza compounds containing pyridine evaluated as novel chelating agents in copper(II) and nickel(II) overload," *J. Inorg. Biochem.*, vol. 105, no. 3, pp. 410–419, 2011.

[89] A. S. Fernandes, J. Costa, J. Gaspar, J. Rueff, M. F. Cabral, M. Cipriano, M. Castro,

and N. G. Oliveira, “Development of pyridine-containing macrocyclic copper(II) complexes: potential role in the redox modulation of oxaliplatin toxicity in human breast cells,” *Free Radic Res*, vol. 46, no. 9, pp. 1157–1166, 2012.

[90] A. S. Fernandes, A. Florido, N. Saraiva, S. Cerqueira, S. Ramalhete, M. Cipriano, M. F. Cabral, J. P. Miranda, M. Castro, J. Costa, and N. G. Oliveira, “Role of the Copper (II) Complex Cu [15]pyN5 in Intracellular ROS and Breast Cancer Cell Motility and Invasion,” *Chem Biol Drug*, vol. 86, pp. 578–588, 2015.

[91] L. Hutchinson and R. Kirk, “High drug attrition rates-where are we going wrong?,” *Nat. Rev. Clin. Oncol.*, vol. 8, pp. 189–190, 2011.

[92] J. Bin Kim, R. Stein, and M. J. O. Hare, “Three-dimensional in vitro tissue culture models of breast cancer – a review,” *Breast Cancer Res. Treat.*, no. 85, pp. 281–291, 2004.

[93] A. L. Correia and M. J. Bissell, “The tumor microenvironment is a dominant force in multidrug resistance,” *Drug Resistance Updates*, 2012. .

[94] M. A. dit Faute, L. Laurent, D. Ploton, M.-F. Poupon, J.-C. Jardillier, and H. Bobichon, “Distinctive alterations of invasiveness, drug resistance and cell-cell organization in 3D-cultures of MCF-7, a human breast cancer cell line, and its multidrug resistant variant.,” *Clin. Exp. Metastasis*, vol. 19, no. 2, pp. 161–8, Jan. 2002.

[95] V. M. Weaver, O. W. Petersen, F. Wang, C. a Larabell, P. Briand, C. Damsky, and M. J. Bissell, “Reversion of the malignant phenotype of human breast cells in three-dimensional culture and in vivo by integrin blocking antibodies.,” *J. Cell Biol.*, vol. 137, no. 1, pp. 231–45, Apr. 1997.

[96] M. Vinci, S. Gowan, F. Boxall, L. Patterson, M. Zimmermann, W. Court, C. Lomas, M. Mendiola, D. Hardisson, and S. a Eccles, “Advances in establishment and analysis of three-dimensional tumor spheroid-based functional assays for target validation and drug evaluation,” *BMC Biol.*, vol. 10, no. 1, p. 29, Jan. 2012.

[97] H. R. Mellor, D. J. P. Ferguson, and R. Callaghan, “A model of quiescent tumour microregions for evaluating multicellular resistance to chemotherapeutic drugs.,” *Br. J. Cancer*, vol. 93, no. 3, pp. 302–309, 2005.

[98] G. Francia, S. Man, B. Teicher, L. Grasso, and R. S. Kerbel, “Gene Expression Analysis of Tumor Spheroids Reveals a Role for Suppressed DNA Mismatch Repair in Multicellular Resistance to Alkylating Agents,” *Mol. Cell. Biol.*, vol. 24, no. 15, pp. 6837–6849, 2004.

[99] A. Ivascu and M. Kubbies, “Diversity of cell-mediated adhesions in breast cancer spheroids,” *Int. J. Oncol.*, vol. 31, no. 6, pp. 1403–1413, 2007.

[100] M. A. Abboodi, “Isolation, identification, and spheroids formation of breast cancer stem

cells, therapeutics implications," *Clin. Cancer Investig. J.*, vol. 3, no. 4, pp. 322–325, Jan. 2014.

[101] Q. Li, C. Chen, A. Kapadia, Q. Zhou, M. K. Harper, J. Schaack, and D. V LaBarbera, "3D models of epithelial-mesenchymal transition in breast cancer metastasis: high-throughput screening assay development, validation, and pilot screen.," *J. Biomol. Screen.*, vol. 16, no. 2, pp. 141–54, Feb. 2011.

[102] A. Beliveau, J. D. Mott, A. Lo, E. I. Chen, A. a. Koller, P. Yaswen, J. Muschler, and M. J. Bissell, "Raf-induced MMP9 disrupts tissue architecture of human breast cells in three-dimensional culture and is necessary for tumor growth in vivo," *Genes Dev.*, vol. 24, no. 24, pp. 2800–2811, 2010.

[103] J. Alcaraz, R. Xu, H. Mori, C. M. Nelson, R. Mroue, V. a Spencer, D. Brownfield, D. C. Radisky, C. Bustamante, and M. J. Bissell, "Laminin and biomimetic extracellular elasticity enhance functional differentiation in mammary epithelia.," *EMBO J.*, vol. 27, no. 21, pp. 2829–2838, 2008.

[104] M. Vinci, S. Gowan, F. Boxall, L. Patterson, M. Zimmermann, W. Court, C. Lomas, M. Mendiola, D. Hardisson, and S. A. Eccles, "Advances in establishment and analysis of three-dimensional tumor spheroid-based functional assays for target validation and drug evaluation," *BMC Biol.*, vol. 10, no. 1, p. 29, 2012.

[105] K. L. Sodek, T. J. Brown, and M. J. Ringuette, "Collagen I but not Matrigel matrices provide an MMP-dependent barrier to ovarian cancer cell penetration.," *BMC Cancer*, vol. 8, p. 223, 2008.

[106] P.-A. Vidi, M. J. Bissell, and S. A. Lelièvre, "Three-Dimensional Culture of Human Breast Epithelial Cells: The How and the Why," *Methods Mol Biol*, vol. 945, pp. 193–219, 2013.

[107] M. Bissell, "Microenvironmental regulators of tissue structure and function also regulate tumor induction and progression: the role of extracellular matrix and its degrading enzymes," *Cold Spring Harb. Symp Quant Biol*, vol. 70, pp. 343–356, 2005.

[108] A. L. Howes, R. D. Richardson, D. Finlay, and K. Vuori, "3-Dimensional culture systems for anti-cancer compound profiling and high-Throughput screening reveal increases in EGFR inhibitor-mediated Cytotoxicity compared to monolayer culture systems," *PLoS One*, vol. 9, no. 9, 2014.

[109] T. Kobayashi, J. Kishimoto, S. Hattori, H. Wachi, H. Shinkai, and E. Burgeson Robert, "Matrix Metralloproteinase-9 Expression Is Coordinately Modulated By the Kre-M9 and Tpa Responsive Elements," *Connect. Tissue*, vol. 34, no. 1, p. 71, 2002.

[110] C.-C. Liang, A. Y. Park, and J.-L. Guan, "In vitro scratch assay: a convenient and inexpensive method for analysis of cell migration in vitro.," *Nat. Protoc.*, vol. 2, no. 2, pp. 329–33, Jan. 2007.

[111] A. Ivascu and M. Kubbies, “Rapid generation of single-tumor spheroids for high-throughput cell function and toxicity analysis.,” *J. Biomol. Screen.*, vol. 11, no. 8, pp. 922–32, Dec. 2006.

[112] H. K. Kleinman and G. R. Martin, “Matrigel : Basement membrane matrix with biological activity,” vol. 15, pp. 378–386, 2005.

[113] Y. Imamura, T. Mukohara, Y. Shimono, Y. Funakoshi, N. Chayahara, M. Toyoda, N. Kiyota, S. Takao, S. Kono, T. Nakatsura, and H. Minami, “Comparison of 2D- and 3D-culture models as drug-testing platforms in breast cancer,” *Oncol. Rep.*, vol. 33, no. 4, pp. 1837–1843, 2015.

[114] J. Y. Fang, S.-J. Tan, Y.-C. Wu, Z. Yang, B. X. Hoang, and B. Han, “From competency to dormancy: a 3D model to study cancer cells and drug responsiveness,” *J. Transl. Med.*, vol. 14, no. 1, p. 38, 2016.

[115] W. Senkowski, X. Zhang, M. Hägg Olofsson, R. Isacson, U. Höglund, M. Gustafsson, P. Nygren, S. Linder, R. Larsson, and M. Fryknäs, “Three-dimensional cell culture-based screening identifies the anthelminthic drug nitazoxanide as a candidate for treatment of colorectal cancer.,” *Mol. Cancer Ther.*, no. November, 2015.

[116] B. J. Kim, S. Zhao, R. P. Bunaciu, A. Yen, and M. Wu, “A 3D in situ cell counter reveals that breast tumor cell (MDA-MB-231) proliferation rate is reduced by the collagen matrix density,” *Biotechnol. Prog.*, vol. 31, no. 4, pp. 990–996, 2015.

[117] L. Xing, M. Hung, T. Bonfiglio, D. G. Hicks, and P. Tang, “Breast Cancer : Basic and Clinical Research The Expression Patterns of ER , PR , HER2 , CK5 / 6 , EGFR , Ki-67 and AR by Immunohistochemical Analysis in Breast Cancer Cell Lines,” *Breast Cancer Basic Clin. Res.*, vol. 4, pp. 35–41, 2010.

[118] J. I. Herschkowitz, K. Simin, V. J. Weigman, I. Mikaelian, J. Usary, Z. Hu, K. E. Rasmussen, L. P. Jones, S. Assefnia, S. Chandrasekharan, M. G. Backlund, Y. Yin, A. I. Khramtsov, R. Bastein, J. Quackenbush, R. I. Glazer, P. H. Brown, J. E. Green, L. Kopelovich, P. a Furth, J. P. Palazzo, O. I. Olopade, P. S. Bernard, G. a Churchill, T. Van Dyke, and C. M. Perou, “Identification of conserved gene expression features between murine mammary carcinoma models and human breast tumors.,” *Genome Biol.*, vol. 8, no. 5, p. R76, 2007.

[119] A. Prat, J. S. Parker, O. Karginova, C. Fan, C. Livasy, J. I. Herschkowitz, X. He, and C. M. Perou, “Phenotypic and molecular characterization of the claudin-low intrinsic subtype of breast cancer.,” *Breast Cancer Res.*, vol. 12, no. 5, p. R68, 2010.

[120] A. Prat and C. M. Perou, “Deconstructing the molecular portraits of breast cancer,” *Mol. Oncol.*, vol. 5, no. 1, pp. 5–23, 2011.

[121] C. J. Lovitt, T. B. Shelper, and V. M. Avery, “Evaluation of chemotherapeutics in a three-dimensional breast cancer model,” *Journal of Cancer Research and Clinical Oncology*, pp. 951–959, 2015.

[122] T. Sethi, R. C. Rintoul, S. M. Moore, a C. MacKinnon, D. Salter, C. Choo, E. R. Chilvers, I. Dransfield, S. C. Donnelly, R. Strieter, and C. Haslett, “Extracellular matrix proteins protect small cell lung cancer cells against apoptosis: a mechanism for small cell lung cancer growth and drug resistance in vivo.,” *Nat. Med.*, vol. 5, no. 6, pp. 662–668, 1999.

[123] B. Weigelt, A. T. Lo, C. C. Park, J. W. Gray, and M. J. Bissell, “HER2 signaling pathway activation and response of breast cancer cells to HER2-targeting agents is dependent strongly on the 3D microenvironment,” *Breast Cancer Res. Treat.*, vol. 122, no. 1, pp. 35–43, 2010.

[124] S. Doublier, D. C. Belisario, M. Polimeni, L. Annaratone, C. Riganti, E. Allia, D. Ghigo, A. Bosia, and A. Sapino, “HIF-1 activation induces doxorubicin resistance in MCF7 3-D spheroids via P-glycoprotein expression: a potential model of the chemo-resistance of invasive micropapillary carcinoma of the breast.,” *BMC Cancer*, vol. 12, no. 1, p. 4, 2012.

[125] Y. Lu, “Cancer cell spheroids for screening of chemotherapeutics and drug-delivery systems,” *Ther. Deliv.*, vol. 6, pp. 1239–1241, 2015.

[126] A. I. Minchinton and I. F. Tannock, “Drug penetration in solid tumours.,” *Nat. Rev. Cancer*, vol. 6, no. 8, pp. 583–592, 2006.

[127] O. Baum, R. Hlushchuk, A. Forster, R. Greiner, P. Clézardin, Y. Zhao, V. Djonov, and G. Gruber, “Increased invasive potential and up-regulation of MMP-2 in MDA-MB-231 breast cancer cells expressing the beta3 integrin subunit.,” *Int. J. Oncol.*, vol. 30, no. 2, pp. 325–32, Feb. 2007.

[128] G. Maity, P. R. Choudhury, T. Sen, K. K. Ganguly, H. Sil, and A. Chatterjee, “Culture of human breast cancer cell line (MDA-MB-231) on fibronectin-coated surface induces pro-matrix metalloproteinase-9 expression and activity,” *Tumor Biol.*, vol. 32, no. 1, pp. 129–138, 2011.

[129] M. Toth and R. Fridman, “Assessment of gelatinases (MMP-2 and MMP-9 by gelatin zymography,” *Metastasis Res. Protoc.*, vol. 57, pp. 1–10, 2001.

[130] L. Alderighi, P. Gans, A. Ienco, D. Peters, A. Sabatini, and A. Vacca, “Hyperquad simulation and speciation (HySS): a utility program for the investigation of equilibria involving soluble and partially soluble species,” *Coord. Chem. Rev.*, vol. 184, no. 1, pp. 311–318, 1999.

[131] Y. Gu, G. Ke, L. Wang, Q. Gu, E. Zhou, Q. He, and S. Wang, “Silencing Matrix Metalloproteinases 9 and 2 Inhibits Human Retinal Microvascular Endothelial Cell Invasion and Migration,” *Ophthalmic Res.*, pp. 70–75, 2015.

[132] N. Hattori, S. Mochizuki, K. Kishi, T. Nakajima, H. Takaishi, J. D'Armiento, and Y. Okada, "MMP-13 Plays a Role in Keratinocyte Migration, Angiogenesis, and Contraction in Mouse Skin Wound Healing," *Am. J. Pathol.*, vol. 175, no. 2, pp. 533–546, 2009.

[133] B. G. Gálvez, S. Matías-Román, J. P. Albar, F. Sánchez-Madrid, and A. G. Arroyo, "Membrane Type 1-Matrix Metalloproteinase is Activated during Migration of Human Endothelial Cells and Modulates Endothelial Motility and Matrix Remodeling," *J. Biol. Chem.*, vol. 276, no. 40, pp. 37491–37500, 2001.

[134] L. J. Mccawley and L. M. Matrisian, "Matrix metalloproteinases : they ' re not just for matrix anymore !," *Curr. Opin. Cell Biol.*, vol. 13, pp. 534–540, 2001.

[135] M. Seiki, H. Mori, M. Kajita, T. Uekita, and Y. Itoh, "Membrane-type 1 matrix metalloproteinase cleaves CD44 and promotes cell migration.," *Biochem. Soc. Symp.*, vol. 153, no. 70, pp. 253–262, 2003.

[136] Y. Hu and L. B. Ivashkiv, "Costimulation of chemokine receptor signaling by matrix metalloproteinase-9 mediates enhanced migration of IFN-alpha dendritic cells.," *J. Immunol.*, vol. 176, no. 10, pp. 6022–33, 2006.

[137] A. L. Correia, H. Mori, E. I. Chen, F. C. Schmitt, and M. J. Bissell, "The hemopexin domain of MMP3 is responsible for mammary epithelial invasion and morphogenesis through extracellular interaction with HSP90β.," *Genes Dev.*, vol. 27, no. 7, pp. 805–17, 2013.

[138] B. Basu, P. Correa de Sampaio, H. Mohammed, M. Fogarasi, P. Corrie, N. a. Watkins, P. a. Smethurst, W. R. English, W. H. Ouwehand, and G. Murphy, "Inhibition of MT1-MMP activity using functional antibody fragments selected against its hemopexin domain," *Int. J. Biochem. Cell Biol.*, vol. 44, no. 2, pp. 393–403, 2012.

[139] A. Dufour, N. S. Sampson, S. Zucker, and J. Cao, "Role of the Hemopexin domain of Matrix Metalloproteinases in Cell Migration," *J. Cell. Physiol.*, vol. 217, no. 3, pp. 643–651, 2008.

[140] E. Millerot-Serrurot, M. Guilbert, N. Fourré, W. Witkowski, G. Said, L. Van Gulick, C. Terryn, J.-M. Zahm, R. Garnotel, and P. Jeannesson, "3D collagen type I matrix inhibits the antimigratory effect of doxorubicin.," *Cancer Cell Int.*, vol. 10, p. 26, 2010.